8-1-1978

Rheological Study of Solvent Refined Lignite Melts

Ajit Venkatraman

RHEOLOGICAL STUDY OF SOLVENT REFINED LIGNITE MELTS

by
Ajit Venkatraman

Bachelor of Technology in Chemical Engineering

Indian Institute of Technology, Madras, India, 1976

A Thesis

Submitted to the Graduate Faculty

of the

University of North Dakota

in partial fulfillment of the requirements

for the degree of

Master of Science

Grand Forks, North Dakota

August
1978

This thesis submitted by Ajit Venkatraman in partial fulfillment of the requirements for the Degree of Master of Science from the University of North Dakota is hereby approved by the Faculty Advisory Committee under whom the work has been done.

Donald E Severson
(Chairman)

David J. Uherka

A M Sonby

Dean of the Graduate School

Permission

Title Rheological Study of Solvent Refined Lignite Melts

Department Chemical Engineering

Degree Master of Science

In presenting this thesis in partial fulfillment of the requirements for a graduate degree from the University of North Dakota, I agree that the Library of this University shall make it freely available for inspection. I further agree that permission for extensive copying for scholarly purposes may be granted by the professor who supervised my thesis work or, in his absence, by the Chairman of the Department or the Dean of the Graduate School. It is understood that any copying or publication or other use of this thesis or part thereof for financial gain shall not be allowed without my written permission. It is also understood that due recognition shall be given to me and to the University of North Dakota in any scholarly use which may be made of any material in my thesis.

Signature Ajit Venkatrao

Date Aug 1, 1978

ACKNOWLEDGEMENTS

The author is very grateful to Professor D. E. Severson for his aid in directing and editing this thesis. Appreciation is extended to Mr. Max Souby for his advice and for consenting to serve as a committee member.

The author also wishes to thank Professor D. J. Uherka for serving as a minor advisor and for his review of the thesis. The author is also indebted to Professor W. R. Kube for his editing of the thesis and for his constructive criticism. Appreciation is also extended to Professor T. C. Owens for his help in providing the graduate assistantship which was of immense help during the author's graduate study in the Department of Chemical Engineering.

The author is also grateful to Mrs. Joanne Maloney for preparing the fine drawings and Mrs. Marlys Kennedy for her efficient typing of the thesis.

TABLE OF CONTENTS

Page

APPENDICES

LIST OF TABLES

LIST OF FIGURES

ABSTRACT

The rheology of solvent refined lignite (SRL) melts was studied using a Brookfield rotational viscometer with a Thermosel system to enable high temperature measurements. The SRL samples were obtained from the Project Lignite process development unit at the University of North Dakota. The effects of temperature cycling, air exposure during heating and continuous shearing over extended periods of time on the viscosity of SRL melts were investigated to develop a suitable method for measuring the viscosities of these melts.

The viscometric data were analyzed for shear dependence and tested using Newtonian, Bingham plastic, and power law models. The Newtonian model was found to describe the behavior of deashed SRL. The behavior of undeashed SRL was described satisfactorily by both the Bingham plastic model and the power law model, although the latter gave a better fit. The power law parameters were correlated with temperature, ash content and melting point of undeashed SRL.

The effects of process variables on the apparent viscosity of undeashed SRL were investigated in detail, and empirical relations were developed in some cases. The process variables studied were conversion temperature, degree of conversion and solvent to coal ratio in the feed to the unit. Temperature was the only process variable found to correlate with the apparent viscosity of undeashed SRL.

The correlation of sample properties such as solvent content, ash concentration, melting point, solid density, molecular weight average with the apparent viscosity of deashed SRL was carried out. Solvent content and melting point of the sample were found to be linearly related to the apparent viscosity of undeashed SRL. Ash concentration and molecular weight average were found to relate to the apparent viscosity by a power greater than one. Density of undeashed SRL was found not to correlate with its apparent viscosity.

The relation between melting point of undeashed SRL and its apparent viscosity was subjected to further investigation. Multiple regression analysis was used to investigate the effect of solvent content, ash content, percent aromatics, percent ethers, percent nitrogen compounds and percent oxy acids on apparent viscosity. Of these, solvent content, percent aromatics and percent ethers were found to affect the apparent viscosity data significantly.

CHAPTER I

INTRODUCTION

The United States has large reserves of coal but only about 20% of the total energy used in this country is derived from coal (1). Oil and gas, which are in significantly smaller supply, account for the bulk of the energy use. To rectify this disparity, the Federal Government is now supporting research to increase coal utilization. One of the consequences of this technology being developed is solvent refining of coal. Solvent refining produces a low melting point fuel by mild hydrogenation, under high pressure. One of the many uses of this refined product is as a clean boiler fuel. Rheology of solvent refined coal is an area of major interest from the point of view of design of equipment and process pipelines.

Vast reserves of lignite exist in western North Dakota. The state and federal government are continually looking at methods of exploiting these reserves. Among the current research programs in this area is the Project Lignite process development unit operated by the University of North Dakota. Interest was expressed in the study of high temperature viscosity of the solvent refined lignite (SRL) product from this facility.

One of the main concerns was to develop a reliable and reproducible technique for measuring the viscosity of hot melts of

SRL. In addition it was also desired that the effects of variables such as ash content, melting point, and solvent content on the viscosity of the product be investigated.

This work was therefore undertaken:

1. To develop a reliable technique for determining viscosity of hot melts of SRL.
2. To propose a model to explain the rheological behavior of SRL, including the effect of temperature and rate of shear.
3. To develop relations between viscosity and sample characteristics such as ash content, solvent content and melting point.
4. To relate viscosity of SRL melts to process variables in the Process Development Unit (PDU), and to determine if viscosity can be employed as a tool in monitoring process operation.

CHAPTER II

TYPES OF VISCOUS BEHAVIOR

Viscosity is a measure of fluid friction. Viscosity is a result of internal friction which occurs when a layer of fluid is made to move in relation to another adjacent layer. A highly viscous fluid possesses a great deal of internal friction. It will not pour or spread as easily as would a material with lesser viscosity (2).

Viscosity can be defined using the following model; consider two parallel layers of fluid of equal area 'A', separated by a distance 'dx', which are moving relative to each other. The force required to maintain the difference in velocity is proportional to the velocity gradient (2).

Expressing this mathematically:

$$\frac{F}{A} = \mu \frac{dv}{dx} \tag{2.1}$$

where $\frac{dv}{dx}$ is the velocity gradient in cm. sec^{-1} $cm.^{-1}$

F is the force in dynes required to maintain the difference in velocity gradient $\frac{dv}{dx}$

and μ is a constant of proportionality in g. sec^{-1} $cm.^{-1}$

This constant of proportionality is referred to as the coefficient of viscosity. The velocity gradient is a measure of the speed at which

the two planes move with respect to each other and describes the shearing experienced by the fluid, which is called rate of shear, 'γ'.

The term $\frac{'F'}{A}$ indicates the force per unit area required to maintain the velocity gradient between the two layers of fluid. It is called the shear stress and is denoted by 'τ'.

Therefore, viscosity can be defined as

$$\mu = \frac{\tau}{\gamma} = \frac{\text{Shear stress}}{\text{Rate of shear}}$$

When this ratio is constant for varying stresses and rates, the fluid is called 'Newtonian'. Thus for a Newtonian fluid the plot of shear stress verses rate of shear will be a straight line passing through the origin (2).

Unfortunately many of the materials used in industry do not behave in the above manner. Such materials are termed 'non-Newtonian' fluids. Many 'non-Newtonian' fluids exist. The types of non-Newtonian fluids are discussed below.

One type of 'non-Newtonian' behavior is called plastic flow. A material exhibiting this phenomenon does not flow until the applied shear stress exceeds a certain value. After this value is exceeded the material follows a behavior similar to that of a Newtonian fluid (2).

Another type is psuedo-plastic flow. In this case the viscosity of the substrate decreases with increasing rate of shear. Essentially these fluids "thin" when sheared (2).

Fluids which show increasing viscosity with increasing rate of shear are called dilatant fluids. These fluids thicken when agitated or stirred.

Thixotropy is another type of 'non-Newtonian' behavior often exhibited by some paints and printing inks. This property is quite similar to the psuedo-plastic except that when shearing is stopped the substance again thickens. This property has been explained as a gel-sol-gel transition. A thixotropic material by definition is a gel that is seemingly liquefies on stirring but returns to a gel state at rest. Such a substance exhibits a hysteresis type of behavior in its shear stress - shear rate relationship (2).

CHAPTER III

MATHEMATICAL MODELS FOR VISCOUS BEHAVIOR

The problem of the rheological behavior of solid melts, as in the present case of SRL, is that non-Newtonian flow is exhibited. In this section, theoretical equations representing non-Newtonian flow are presented and methods for correlating viscosity with ash content and other properties of the SRL are developed.

1. Shear Dependence of Viscosities of Solid Melts

It has been pointed out by Van Wazer *et al.* (3) that most solid melts and macro-molecular substances tend to exhibit psuedo-plastic behavior. Since SRL is composed of substances with different molecular weights, starting from the lower molecular weight solvent, which is essentially Newtonian, to the high molecular weight asphaltenes, which are definitely non-Newtonian, it becomes necessary to consider the theoretical equations for the different types of fluid behavior that were discussed in Chapter II.

The Newtonian behavior can be mathematically expressed as

$$\tau = - \mu_o \gamma \qquad (3.1)$$

where τ is the shear stress in dynes cm.$^{-2}$,

μ_o is the viscosity in poises (gm cm.$^{-1}$ sec^{-1}), and

γ is the shear rate in sec^{-1}.

Hence for a Newtonian fluid, viscosity is independent of shear rate.

The Bingham plastic model can be represented by the following equation,

$$\tau = -\mu_p \gamma + \tau_o \qquad (3.2)$$

where μ_p is the plastic viscosity of the fluid in poises.

τ_o is the yield stress for the fluid in dynes cm.$^{-2}$.

This model is commonly used to describe the behavior of suspensions, for example that of nuclear fuels in heavy water (4).

Another equation describing non-Newtonian flow is the power law model given by:

$$\tau = m \gamma^n \qquad (3.3)$$

where 'm' and 'n'; are power law parameters; 'n' is dimensionless whereas 'm' has units of gm cm^{-1} sec^{-n}. Shaheen (5) found this model to fit concentrated suspensions of styrene-divinyl benzene beads in water. Mishra (6) found that this model fitted the data for concentrated silica suspensions in water.

Many other non-Newtonian models have been proposed, the prominent ones being the power law model with a yield stress, the Eyring model, the Ellis model and the Reiner-Philipoff model, details of which can be obtained from Van Wazer et. al. (3).

A graphic representation of the different types of fluids is given in Figure 1.

2. Rotational Viscometry and Torque Versus Angular Velocity Relationships for Different Fluid Types

When a rotational viscometer, such as the Brookfield viscometer is used to measure viscosity, the fluid is in tangential annular flow

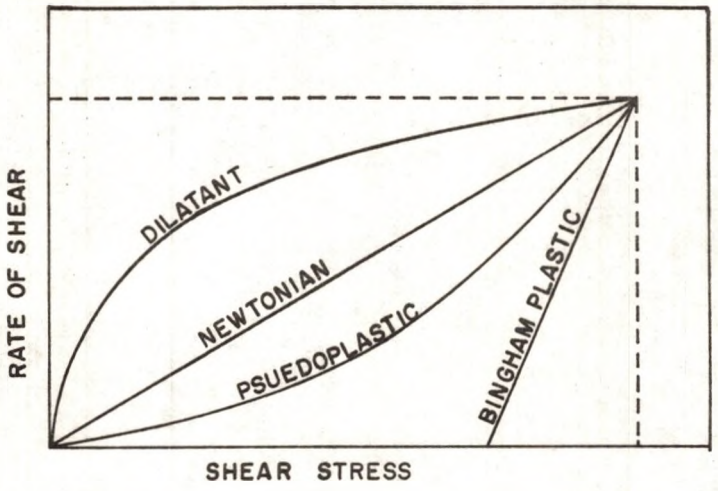

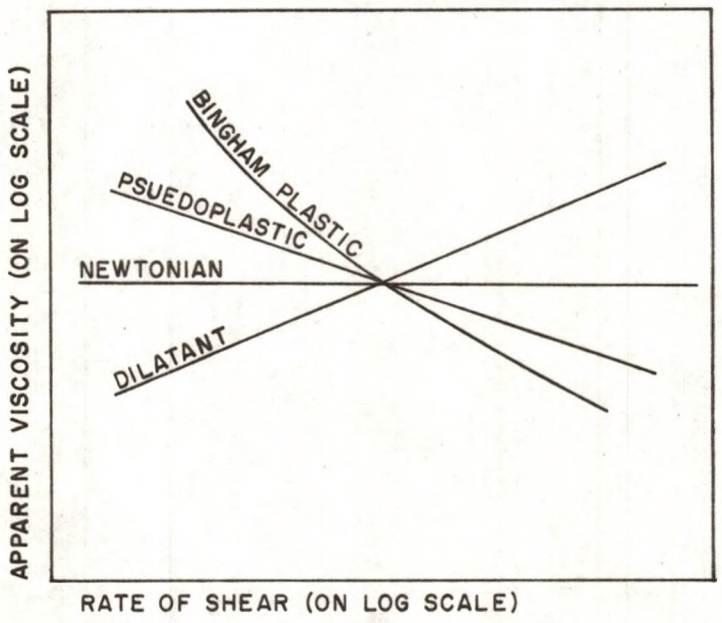

FIGURE 1- SHEAR STRESS - RATE OF SHEAR RELATIONSHIP FOR DIFFERENT FLUIDS

between an inner rotating cylinder and a stationary outside cylinder. The scale reads an apparent viscosity and calibration is based on the torque necessary to maintain the velocity of the rotating cylinder.

If μ is the apparent viscosity reading at an angular velocity of (rad sec^{-1}), then the torque is given by the following equation (7).

$$T = \frac{4\pi h \mu}{(r_1^{-2} - r_2^{-2})} \tag{3.4}$$

where r_1 is the radius of the inner cylinder in cm

r_2 is the radius of the outer cylinder in cm

h is the height of the inner cylinder in cm

T is the torque in the inner cylinder in dyne cm

Appendix A and Appendix B show the derivation of the torque-angular velocity relationship in a rotational viscometer for a Bingham plastic and a power law fluid respectively. For a Bingham plastic the derived relationship is given by equation (3.5)

$$\omega = \frac{T}{4\pi h \mu} (r_1^{-2} - r_2^{-2}) + \frac{\tau o}{\mu} \ln \frac{r_1}{r_2} \tag{3.5}$$

and for a power law fluid, the equation is:

$$\omega = \left(\frac{T}{2\pi hm}\right)^{1/n} \frac{n}{2} (r_1^{-2/n} - r_2^{-2/n}) \tag{3.6}$$

The symbols above have the same meaning as given previously.

CHAPTER IV

RELATED WORK ON COAL LIQUID VISCOSITIES

A great deal of the work done in rheology of coal and coal derived products in the U.S.A. have been conducted by the Energy Research and Development Administration (ERDA) (now the Department of Energy) or under an ERDA contract.

Very little work is reported in current literature in viscosity studies of hot melts of coal derived products, but a great deal of work has been done on non-Newtonian fluids in general, and particularly in the case of polymers, adhesives, paints and glass.

Huang et. al. (8) have done studies on the viscosities of Synthoil, a coal derived product, and have reported that small amounts of additives of Dupont surfactants are capable of reducing viscosities of Synthoil by about 11 per cent.

Theoretical and experimental work is now in progress at the University of Michigan to develop a method to measure viscosities of coal liquids at high temperature and pressure. Results are yet to be reported (9).

Knell et. al. (10) have done studies on coal tar viscosity in relation to reactor variables like residence time and temperature of reaction. According to them, tar viscosity is lowered when residence time is increased. This was found to be true at all of the three temperatures at which these studies were made.

Klunder et. al. (11) have reported on viscosities of coal slurries in relation to coal concentration. Vehicle used was zinc chloride in water solution.

The viscosities of coal liquids and petroleum heavy ends have been the subject of some investigation during the past year, and the effect of asphaltene content has shown to be important (12). Coal derived oils and petroleum oils which contained 10 to 30 percent asphaltenes showed a marked increase in viscosity with increasing concentrations of asphaltenes. (Asphaltenes are defined as that fraction which is soluble in benzene but insoluble in hexane.) Burk et. al. (13) have shown that molten asphaltenes exhibited a lower viscosity than do molten preasphaltenes at the same temperature. (Preasphaltenes are defined as that fraction which is insoluble in benzene but soluble in pyridine.) Solution viscosity of Athabasca asphaltenes has been investigated by Moschpedis et. al. (14).

Schiller et. al. (15) found the viscosity of simulated coal liquids to relate very well with properties such as molecular weight, oxygen content, concentration of weak acids and hexane soluble constituents. In their study, it was also found that mass spectral data, concentration of weak bases, and concentration of asphaltenes have greater effect on increasing viscosity than do comparable concentrations of asphaltenes in coal liquids.

CHAPTER V

SCOPE OF PRESENT WORK

The present work is the investigation of the rheological properties of SRL at elevated temperatures. The present study comprises three parts.

A) Development of a method of determining the viscosity of SRL at temperatures to 500^{o}F using a Brookfield viscometer. The method developed should be simple, reproducible, reliable and relatively inexpensive.

B) Proposal of a mathematical model to describe the behavior of SRL melts. The model proposed should be simple, in that not more than three parameters should be necessary to explain viscosity relationships of SRL.

C) Investigation of the effect of ash content, solvent content, temperature, and density of SRL on its viscosity. Regression analysis will be undertaken to obtain coefficients for empirical relations between viscosity and the variables.

Results should provide information which will help in the design of process pipelines and equipment. This study should also help in the employment of viscosity as a control for monitoring process operations.

CHAPTER VI

MATERIALS, APPARATUS AND EXPERIMENTAL PROCEDURES

This chapter includes details of the materials, the apparatus, and the experimental procedures used in this work.

MATERIALS.

The solvent refined lignite samples were obtained from the Project Lignite pilot plant. This plant was constructed and is operated by the University of North Dakota, under federal sponsorship. Solvent refining converts lignites (or other coals) into low ash, high heat content, low sulfur, "clean" fuels for use in power plants.

Lignite is first pulverized and then blended into a slurry with a petroleum derived solvent. The slurry is preheated after mixing with compressed carbon monoxide and hydrogen. The preheated mixture goes to a dissolver where coal depolymerization and hydrogenation take place. The mineral content of the coal remains undissolved. The gases and light oils are separated from the slurry in three flash vaporization steps. The gas is then purified and part of the cleaned gas is recycled to the dissolver. The light oils consist of the original solvent, hydrocarbons and phenols. Recovered solvent is recycled to form slurry with the feed lignite. The residue from the flash vaporization consists of mineral residue,

undissolved lignite and solvent refined lignite and is referred to as vacuum bottoms. The vacuum bottoms are pumped to a mixing loop at about 400°F and mixed with toluene under pressure. The mixture is then pumped to a gravity settler where undissolved mineral residue and unreacted lignite are removed as solids. The dissolved SRL and toluene are withdrawn from the top of the settler. Toluene is then removed and recycled, and the SRL is solidified and collected.

Deashed and undeashed SRL samples from the plant were analyzed for ash content, pyridine solubility, and melting point. Samples used for viscosity measurements were selected so that they differed appreciably in ash content and pyridine solubilities and melting point. Samples were obtained in the above manner from four different runs of the plant.

Sample group I was obtained from Project Lignite run No. SDR-5. This group includes only one sample, not deashed, which will be referred to as sample I. Complete analysis of sample I is given in Table 1 , Appendix C.

Sample group II was obtained from Project Lignite run No. M-11. This group also includes only one sample which was deashed and will be referred to as sample II. Sample II analysis is given in detail in Table 2 , Appendix C.

Sample group III includes nine samples which were obtained from run No. M-29. This run lasted seven days and had nine yield periods at intervals of twelve hours each. The samples in this group, not deashed, are essentially the products obtained during

these yield periods, and will be referred to as samples III A, III B, III C etc.

Samples of group IV were obtained from run No. L-1 of the Project Lignite pilot plant. Run No. L-1 lasted for a month and samples were obtained at random time intervals. Twenty such samples were used for viscosity measurements and will be referred to as IV A, IV B, and etc.

TABLE 1

PROPERTIES OF SAMPLES STUDIED

Sample Group	Obtained from PDU Run	No. of Samples in Group	Ash content (wt. %)	Remarks
I	SDR-5	1	8.0	
II	M-11	1	0	Deashed
III	M-29	9	8.9-11.6	Extracted at 12 hour intervals
IV	L-1	20	10.7-13.0	Spot samples at random intervals

Total No. of Samples = 31

Samples used in viscosity measurements were analyzed for solvent content, tetrahydrofuran (THF) solubility, average molecular weight by vapor pressure osmometry, percent aliphatics, percent ethers, percent nitrogen compounds and percent oxy acids by the Grand Forks

Energy Research Center, Department of Energy. A summary of these analyses is given in Table 5 , Appendix C. Nitrogen used in this work was obtained from the Dow Supply Company and was of dry grade, high purity.

APPARATUS.

The apparatus used for apparent viscosity measurement was a Brookfield Synchro-Lectric Viscometer with a Thermosel system to enable high temperature viscosity measurements. The Brookfield Thermosel system permits viscosity measurements up to 500 F, with a 1 percent reproducibility (2). Viscometer specifications are given in Appendix D. Viscosity measurements are made using co-axial cylinder geometry. Temperature is controlled using a full wave proportional controller which maintains the spindle and sample at the desired temperature. Complete Thermosel specifications are given in Appendix D. The basic components of the equipment used for viscosity measurements are:

1. A Brookfield Synchro-Lectric Viscometer.
2. A thermo-container, which is used to heat the sample.
3. A removable sample chamber and spindle.
4. A full wave proportional temperature controller.

Specific gravities of the samples were measured using a pycnometer, with kerosene as the displacement medium. Sample specific gravity measurements are given in Appendix E.

EXPERIMENTAL PROCEDURE.

Solvent refined lignite samples were first pulverized to a fine powder using a pestle and mortar. A 10.5 gram sample was weighed out and transferred to a clean and dry sample chamber. Care was taken to avoid compacting the sample. The Thermo-container was cleaned, and the probe from the temperature controller was inserted into the receptacle at the back of the Thermo-container. The Thermo-container was then plugged into the output of the controller. The set point dial on the controller was set at the desired temperature and the proportional band and manual reset knobs were both turned counter-clockwise to a minimum.

The viscometer was mounted on its stand and levelled using the three levelling screws on the base, the appropriate spindle inserted, and the alignment bracket attached. The viscometer was then lowered so that the spindle was well within the Thermo-container sample holder and the alignment bracket just touched the alignment ring on top of the Thermo-container. The temperature controller was then switched on and the spindle was allowed to heat up within the Thermo-container. The heating process was found to take about thirty minutes.

When the temperature of the Thermo-container reached a desired value (as indicated by the pointer on the deviation meter remaining steady at zero), the spindle was raised and the sample chamber containing the powdered sample was lowered into the well of the Thermo-container. The spindle was then lowered and aligned as before. Alignment of the spindle was found to be an important

criterion and if not done exactly as indicated could result in erroneous readings. Sample size is also important and it was determined by trial and error that 10.5 grams of solvent refined lignite when heated to between 350° and 500°F would occupy the required volume of 9 ml as stated in the manufacturers literature.

After the spindle was aligned, an insulating cap was placed on top of the sample chamber so that the whole system was capped and thermally insulated from heat losses. The spindle shaft was checked so as to be capable of free rotation, and was then centered in the middle of the hole in the insulating cap.

The knob on the viscometer was set at the highest speed, 60 rpm, and the unit turned on. The rotating spindle served as a stirrer and helped the sample to attain thermal equilibrium quickly. As the sample started to melt some frothing occurred and the sample level was found to rise, because of bubbles escaping to the surface. The spindle was kept rotating at its highest speed, as this was found to decrease the possibility of sample overflow from the chamber.

As the temperature of the sample increased the viscosity was found to decrease and finally reached a steady value when thermal equilibrium was reached. Equilibrium was determined by a steady zero reading on the temperature deviation meter and by a steady dial reading on the viscometer dial. The average time taken to attain thermal equilibrium was from 30 to 45 minutes.

Dial readings were recorded for all possible speeds of the viscometer spindle that gave meaningful readings. All readings were

made within 20 minutes after reaching thermal equilibrium. To show that thixotropy was present to an appreciable degree (within the time measurements were taken) the measurements were made in a random sequence of spindle speeds.

The calibration of the viscometer was checked frequently by measuring the viscosity of the standard solutions, obtained from the manufacturer.

CHAPTER VII

RESULTS AND DISCUSSION

In this part of the paper, the analyses of the results are presented. Table 13 in Appendix F gives the complete apparent viscosity data. A sample calculation of torque and angular velocity is given in Appendix G. Appendix H gives the complete torque-angular velocity data. Calculations of the power law parameters are presented in Appendix I.

Development of Technique for Measurement of Viscosity SRL Melts

1. Non-Newtonian Behavior of a Typical SRL Melt (Undeashed).

The apparent viscosity of a typical SRL undeashed melt shows a definite shear dependence. Fig. 2 is a plot of the apparent viscosity of sample III-E as a function of shear rate. The figure shows that the apparent viscosity decreases with increasing shear rate, indicating non-Newtonian behavior.

2. Effect of Temperature Cycling on SRL Apparent Viscosity.

The viscosity of a SRL melt at a given temperature changes due to temperature cycling over a period of time. Fig. 3 shows the effect of temperature cycling on the apparent viscosity of sample II. The apparent viscosity data for this plot is reported at an angular velocity of 12 rpm. The figure shows an increase in viscosity at a given temperature with time. This increase in apparent viscosity at a particular temperature can be attributed to

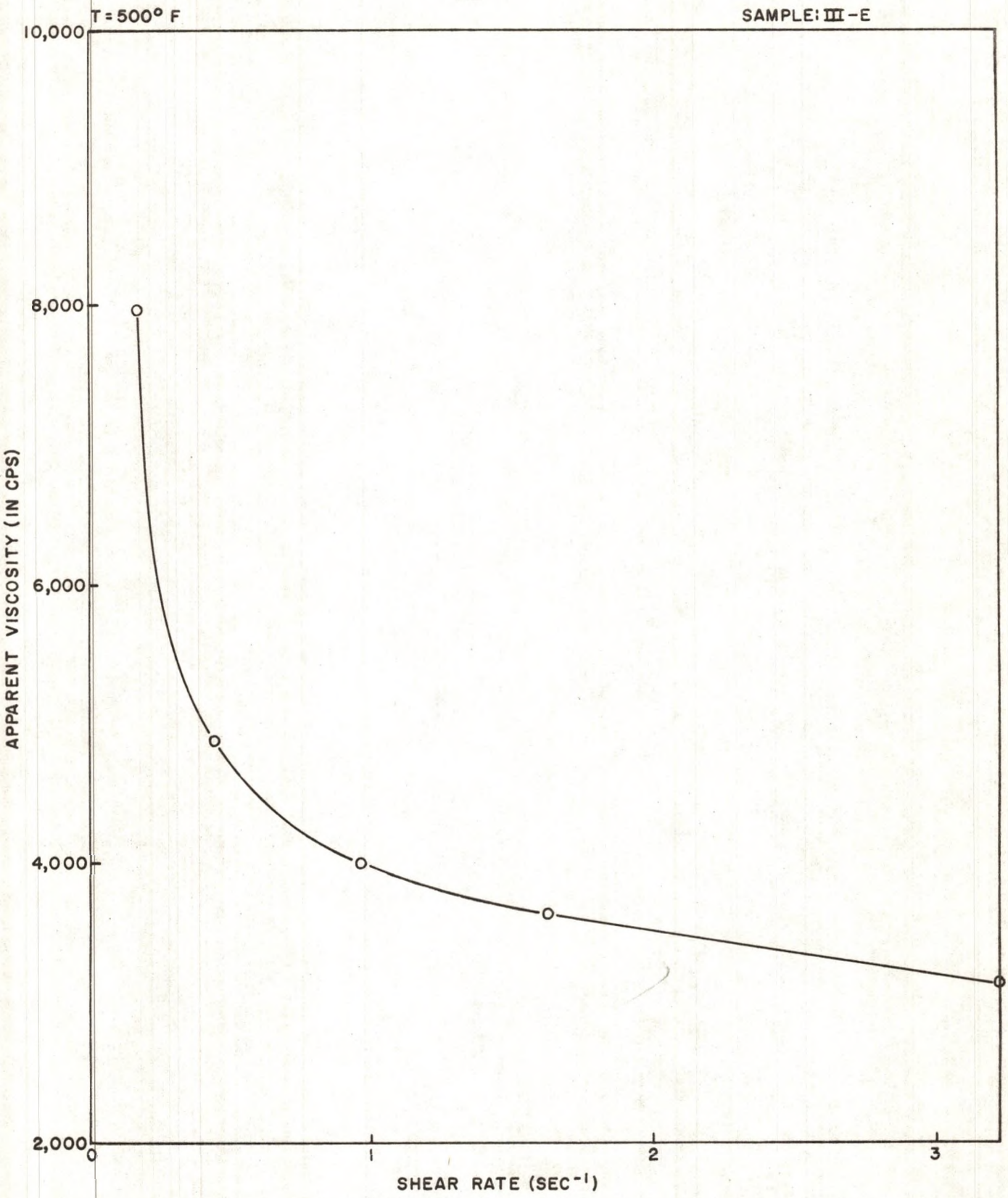

FIGURE 2- NON-NEWTONIAN BEHAVIOR OF A TYPICAL SRL MELT (Undeashed)

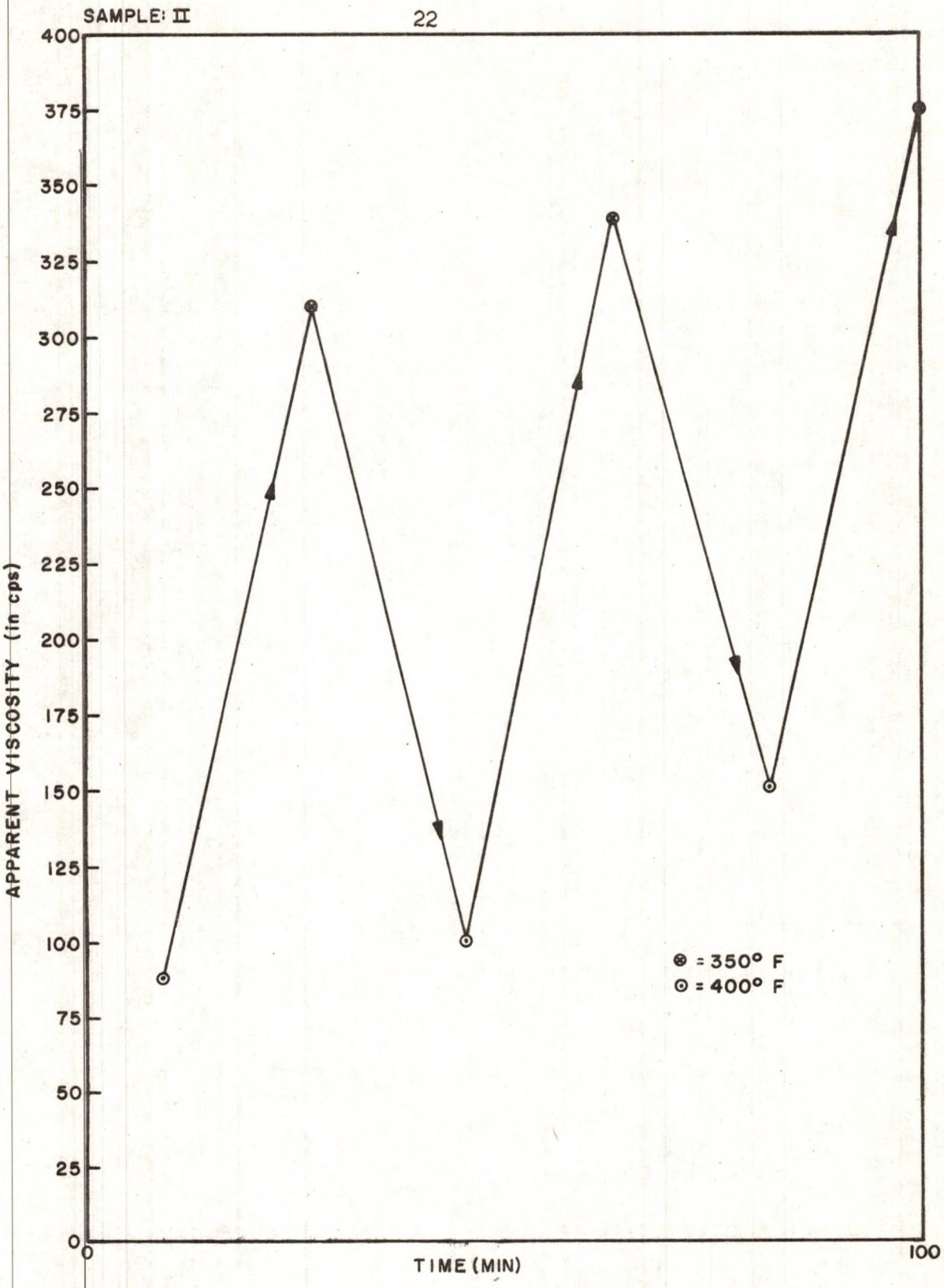

FIGURE 3 - EFFECT OF TEMPERATURE CYCLING ON APPARENT VISCOSITY AT 12 RPM

i) Change in structure of the SRL due to temperature cycling, or

ii) Change in structure of SRL due to continuous heating over a period of time. It can also be seen from the figure that this increase occurs at both the temperatures under consideration. Figures 4 and 5 show a similar behavior of the apparent viscosity of SRL when measured at angular velocities of 30 and 60 rpm respectively. It can be concluded that temperature cycling causes a hysteresis effect on apparent viscosity. This hysteresis effect is lesser at higher angular velocities.

Because the apparent viscosity of an SRL melt exhibits a hysteresis effect on temperature cycling, it was decided to make all further viscosity measurements in a way that minimizes these effects. Hence temperature changes were made in ascending order only.

3. Effect of Continuous Shearing over Extended Periods of Time.

Figure 6 shows the effect of continuous shearing on the apparent viscosity of sample III-A. The first part of the figure shows an initial rapid decrease of apparent viscosity due to the heating of the sample, until a minimum value is attained. This minimum value occurs when the sample has reached the temperature of the controller set point. On continued shearing the apparent viscosity starts to increase, slowly at first and later on rapidly as indicated by the second part of the figure, where the viscosity has been plotted on semi-logarithmic coordinates.

The low point of the curve indicates the time when thermal equilibrium has been attained by the sample, and the SRL is at

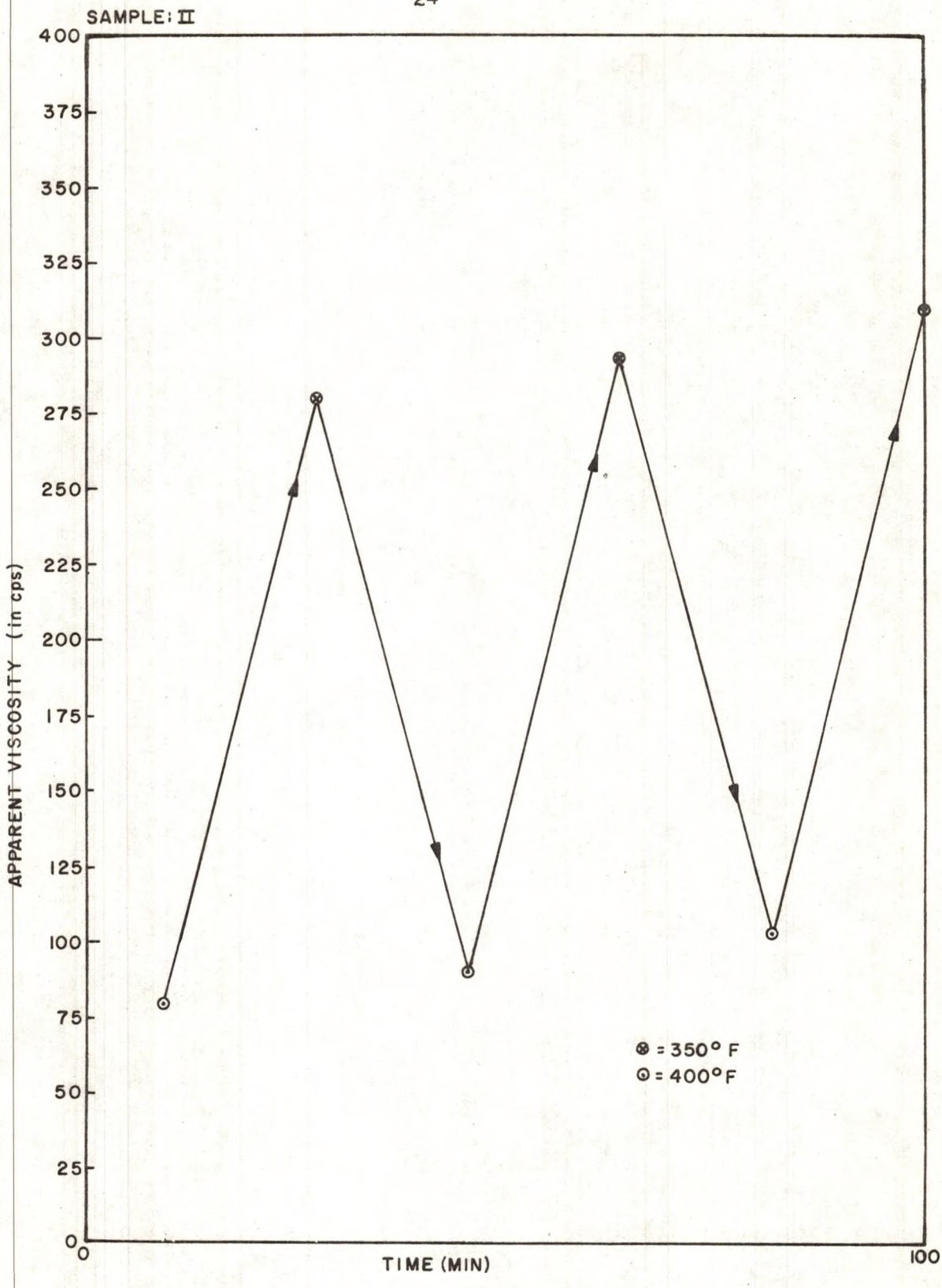

FIGURE 4-EFFECT OF TEMPERATURE CYCLING ON APPARENT VISCOSITY AT 30 RPM

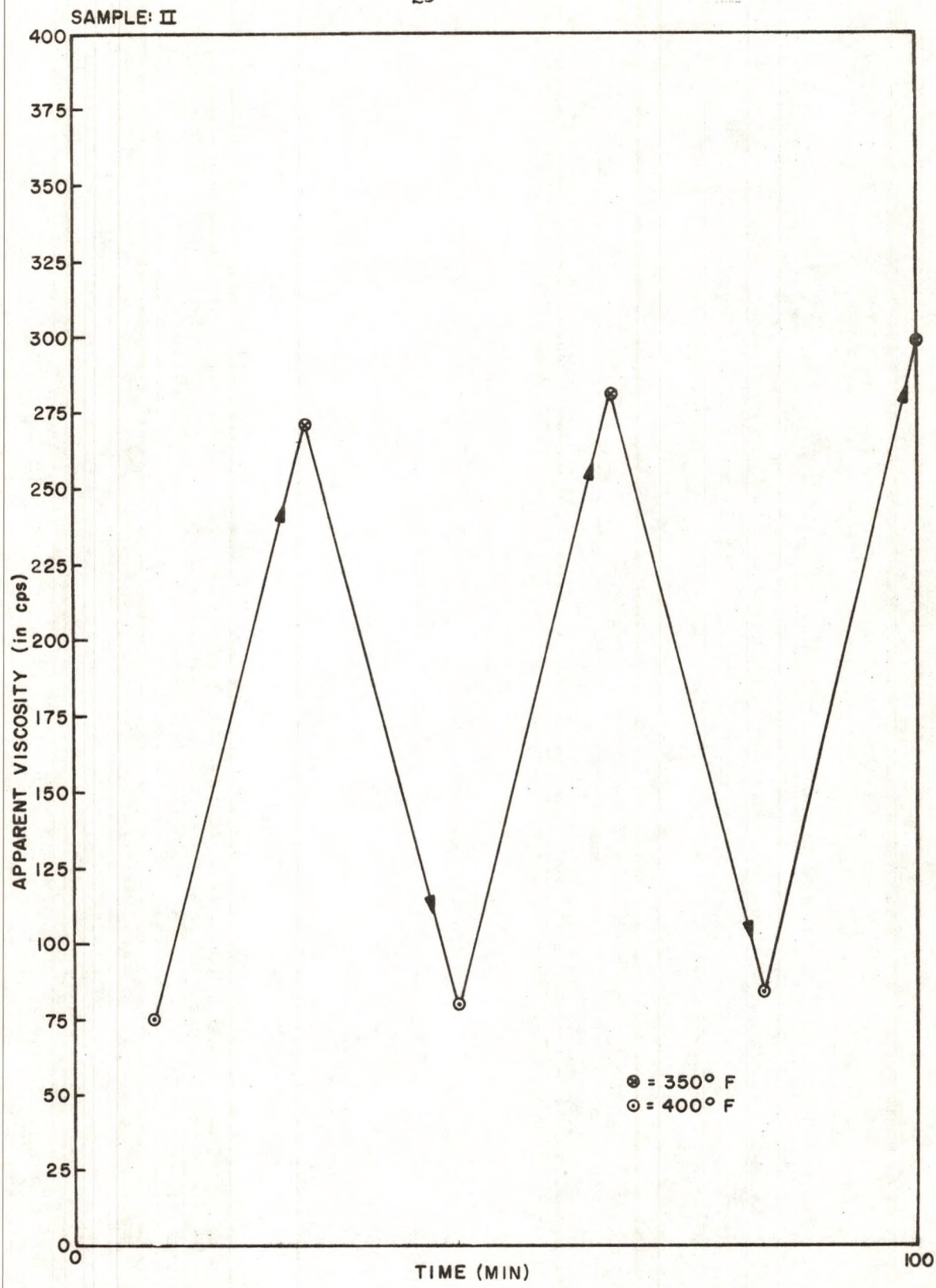

FIGURE 5 - EFFECT OF TEMPERATURE CYCLING ON APPARENT VISCOSITY AT 60 RPM

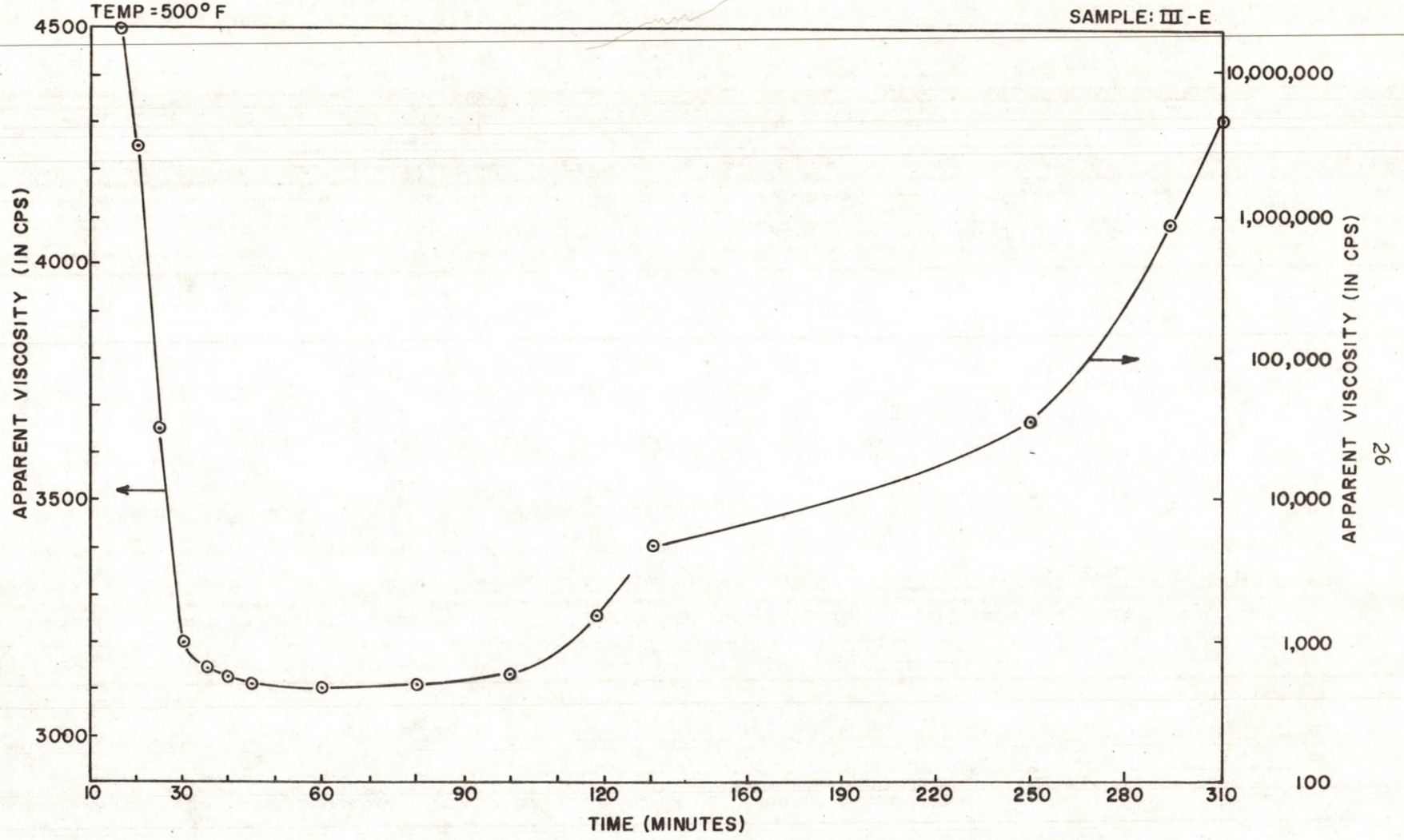

FIGURE 6-EFFECT OF SHEARING OVER EXTENDED PERIODS OF TIME

a constant temperature. All additional viscosity measurements in this report were taken during the time when a sample reached its lowest viscosity; in other words data were taken when a sample reached thermal equilibrium.

4. Effect of Air Exposure on SRL Apparent Viscosity.

The apparent viscosity of SRL increases appreciably on exposure to air at a constant temperature. Figure 7 shows the plot of apparent viscosity of sample III-E, as a function of shear rate with and without nitrogen blanketing. It is evident from the presentation that SRL when exposed to air becomes more viscous than when protected by an inert gas. All later viscosity measurements were made with a nitrogen blanket to avoid exposure of the SRL to air.

Solvent Refined Lignite Viscosity Models

In this section models are used to describe the behavior of deashed and undeashed SRL melts. Apparent viscosity measurements were made at different temperatures to determine if temperature influenced the behavior of SRL melts. Table 3 in Appendix F gives the complete apparent viscosity and shear rate data for these samples.

Plots of torque versus angular velocity were prepared for the different samples. The torque was calculated from equation (3.4) using the apparent viscosity and the geometry of the apparatus. A sample calculation of torque is given in Appendix G. Tables in Appendix F summarize the calculated values of torque and angular velocity.

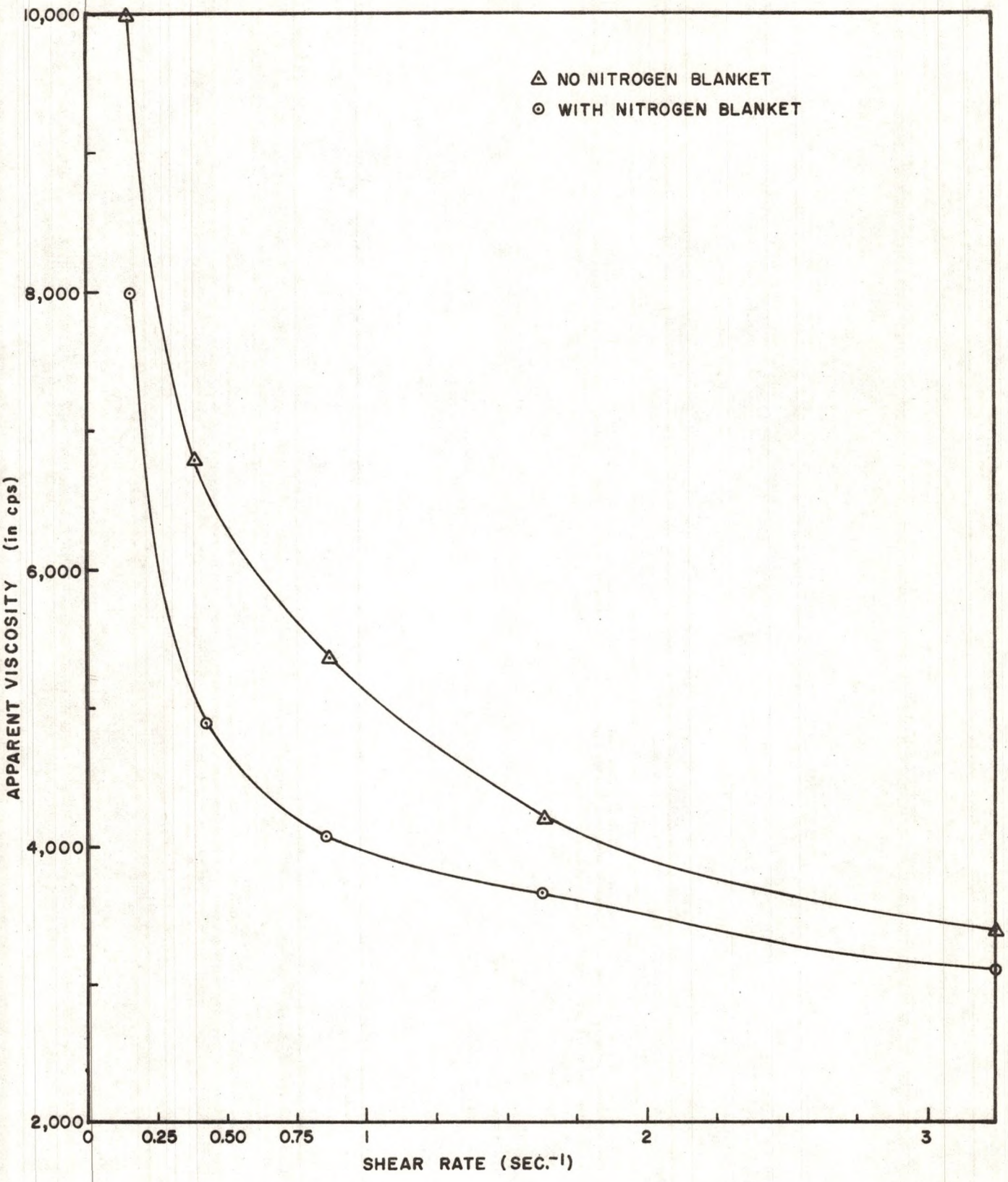

FIGURE 7 - EFFECT OF AIR EXPOSURE ON SRL APPARENT VISCOSITY

1. Newtonian Models for Deashed SRL Melts

Figure 8 shows the torque-angular velocity relationship for deashed SRL (sample II) to be a straight line through the origin, implying that this sample is Newtonian and the viscosity data exhibit behavior in accordance with equation (3.4). The correlation coefficient 'r^2' on the plot is an indication of the percentage of the scattering of the data that can be explained by the straight line. The torque-angular velocity relationship has been plotted at three temperatures and it can be seen that the Newtonian model is satisfactory for most of the data at all three temperatures. The values of 'r^2' indicate that there is lesser deviation from the model at higher temperatures. A possible explanation for this could be that at lower temperatures the SRL may contain suspended solids. Any presence of solid particles thus results in the formation of a suspension which gives a deviation from Newtonian behavior.

2. Non-Newtonian Models for Undeashed SRL Melts

For a Bingham plastic, the torque-angular velocity relationship is a straight line, with slope equal to the plastic viscosity and intercept equal to the yield stress as shown in equation (3,5). In the case of a power law fluid, the torque-angular velocity relationship is a straight line on a logarithmic plot. Regression lines for both models have been drawn on the cartesian coordinates plot. In each case the dotted line is the power law model regression line and was drawn using the power law parameters 'm' and 'n', obtained from the logarithmic plot. Correlation coefficients 'r^2' have been computed to give a quantitative idea of the degree of fit

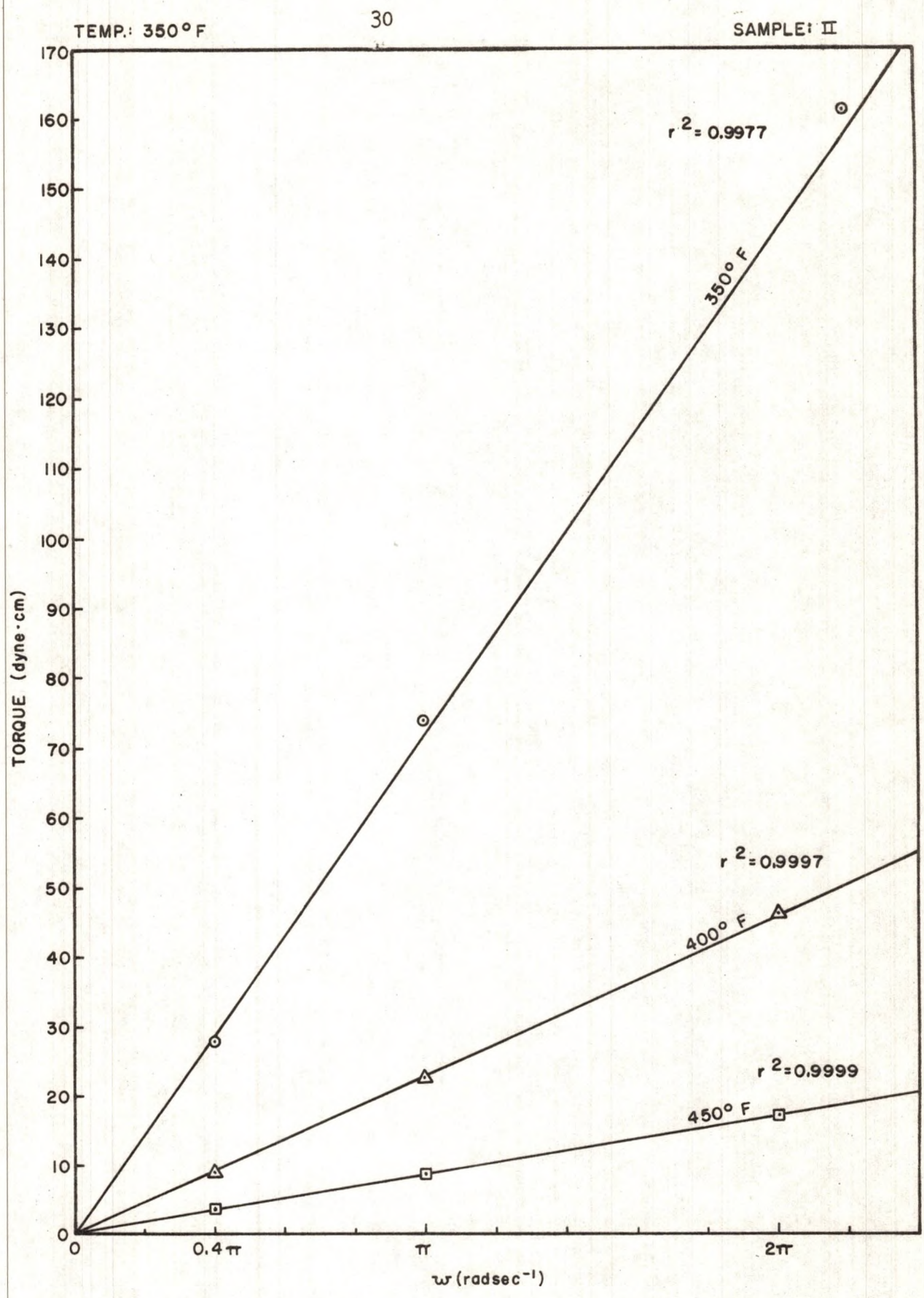

FIGURE 8 - NEWTONIAN BEHAVIOR OF DEASHED SRL

obtained.

Figure 9 is the torque-angular velocity relationship on cartesian coordinates for undeashed SRL (sample I). Data were obtained at temperatures of 440° and 500°F, to see if temperature influenced the behavior of undeashed SRL. The same data are plotted on a logarithmic scale in Figure 10. The data give a better linear relation on the logarithimic plot than on the cartesian plot, implying that the undeashed sample fits the power law model better than the Bingham model. The regression coefficient 'r^2' indicates that in the case of both models the data correlate better at higher temperatures. The same temperature dependence was exhibited by the Newtonian model for deashed SRL.

In Figures 11 and 12 the torque-angular velocity relationships have been plotted for four different samples of group III, to see if the behavior of undeashed SRL is influenced by sample properties. Figure 13 presents the data of Figure 11 on a logarithmic plot. Again the data approximates a straight line more nearly on the logarithmic plot than on the cartesian plot, confirming that undeashed SRL fits the power law model better than the Bingham model. The values of the correlation coefficients indicates that the power law model fits the data closer when the sample melting points are lower. The Bingham model does not give a definite correlation with sample melting point.

Figures 14 through 20 show torque versus angular velocity for undeashed SRL sample IV-T, at six different temperatures. The sample was heated from 350°F to 500°F and apparent viscosity measurements

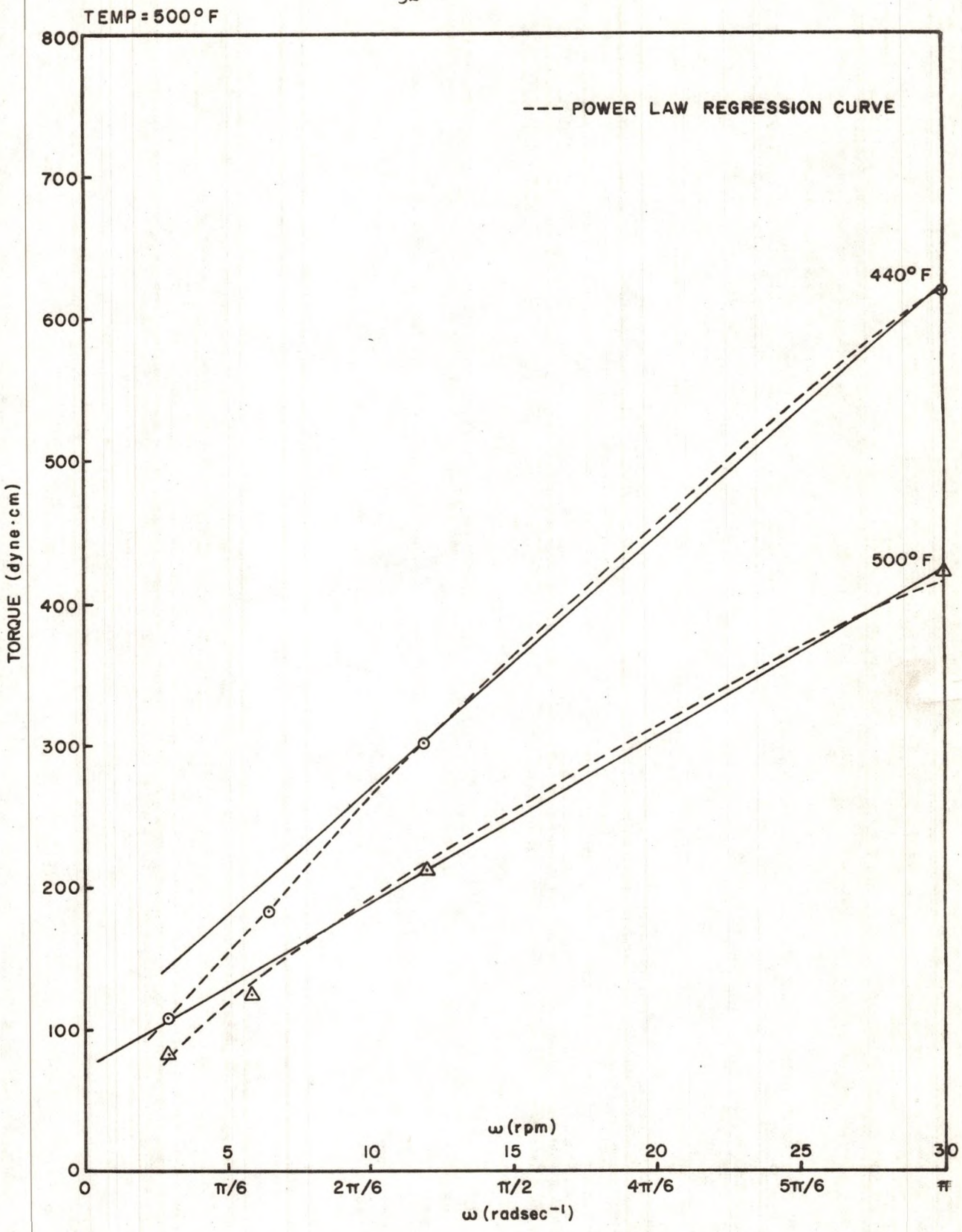

FIGURE 9 - NON-NEWTONIAN MODELS FOR UNDEASHED SRL (Sample I)

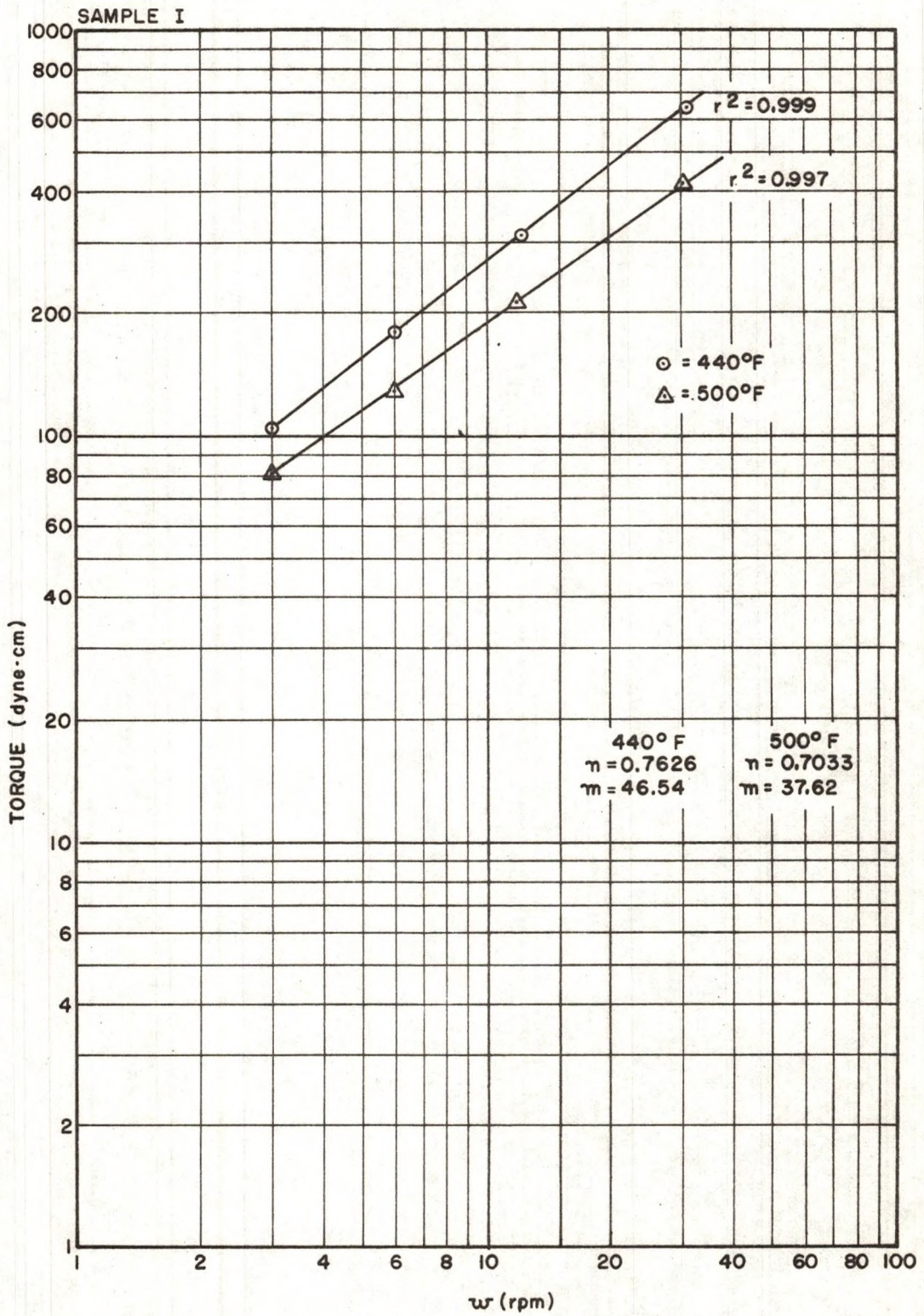

FIGURE 10-TORQUE VERSUS ANGULAR VELOCITY ON LOGARITHMIC CO-ORDINATES

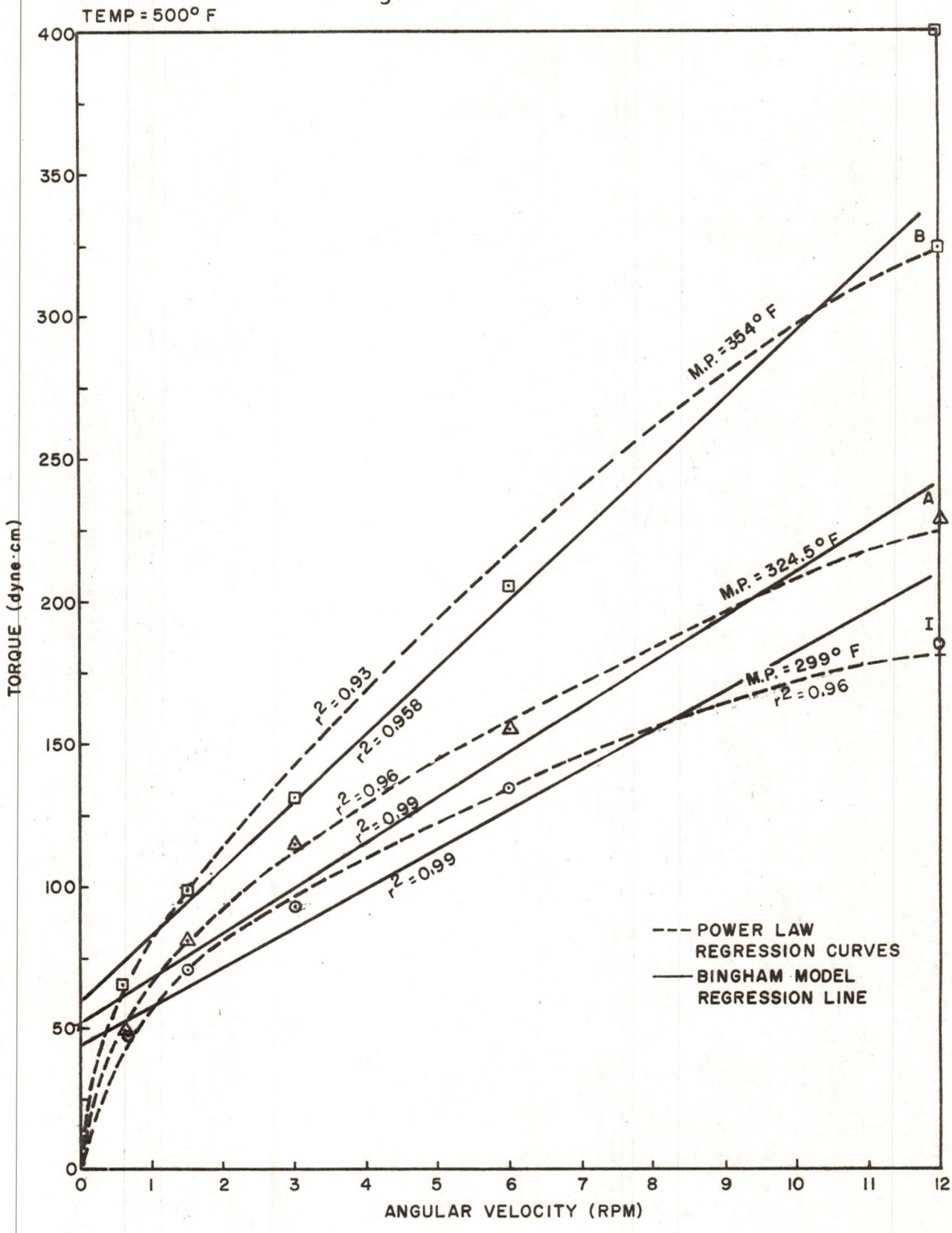

FIGURE II - NON-NEWTONIAN MODELS FOR UNDEASHED SRL (Sample III)

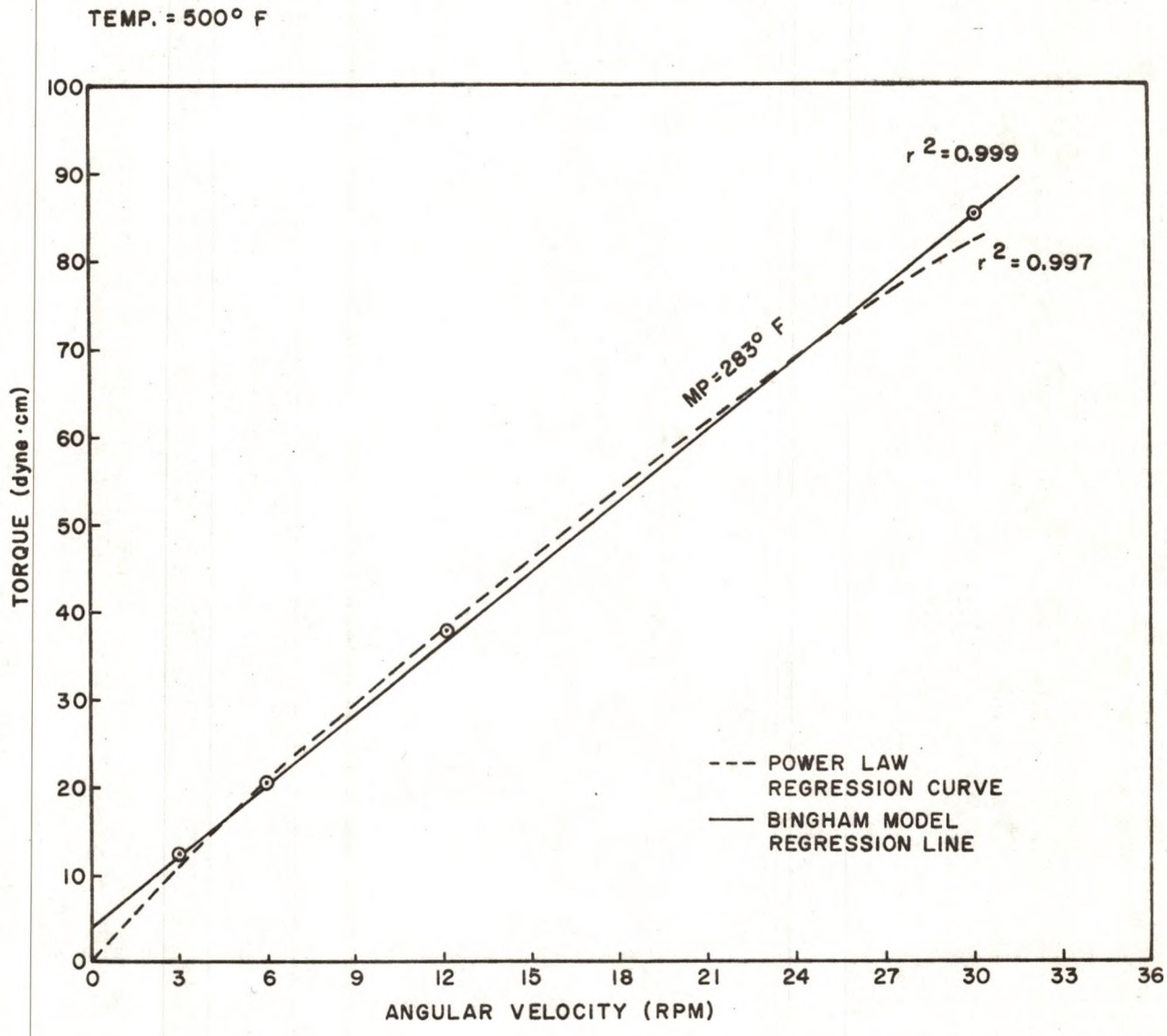

FIGURE 12 - NON-NEWTONION MODELS FOR UNDEASHED SRL
(Sample I, Continued)

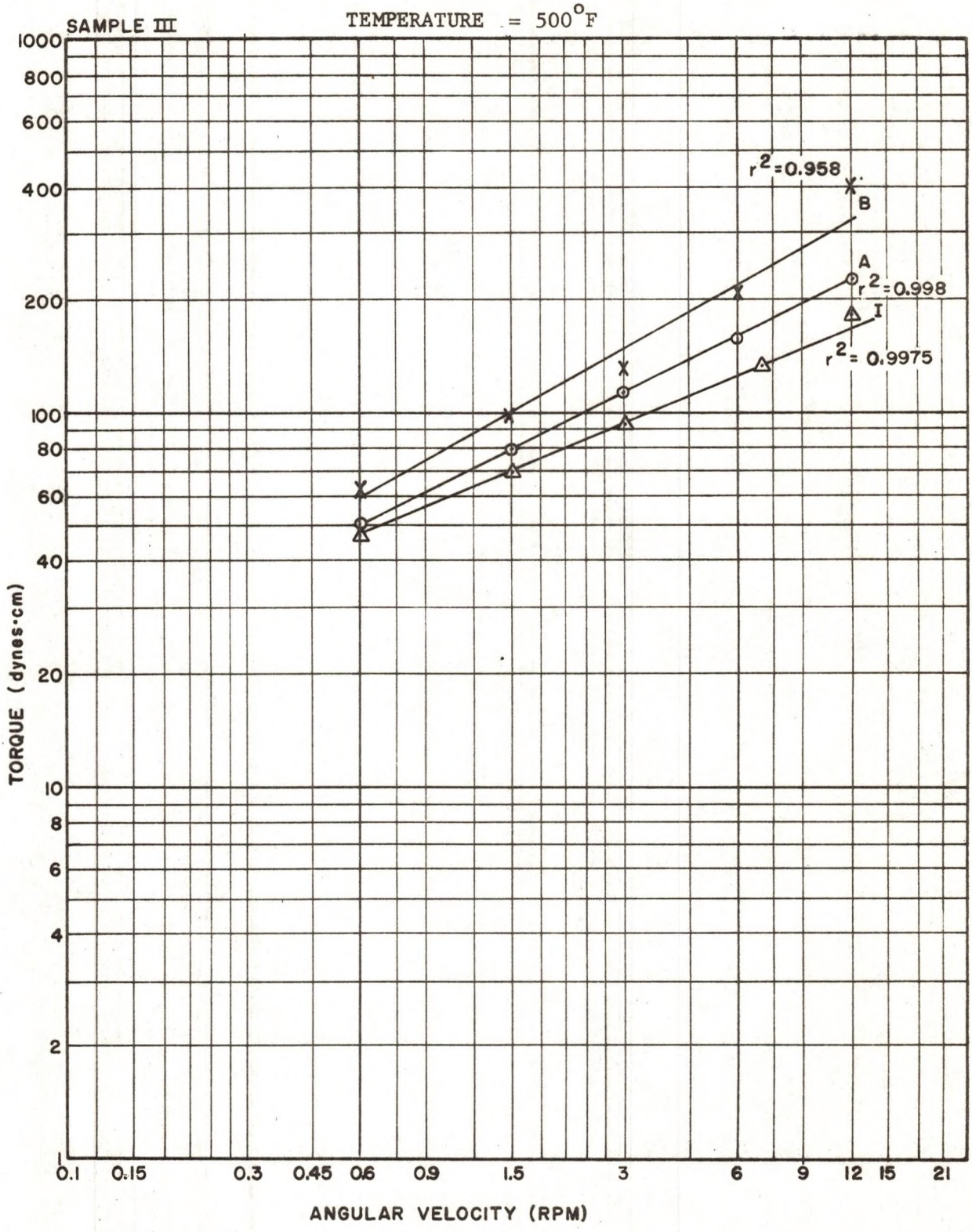

FIGURE 13 - TORQUE VERSUS ANGULAR VELOCITY ON LOGARITHMIC CO-ORDINATES

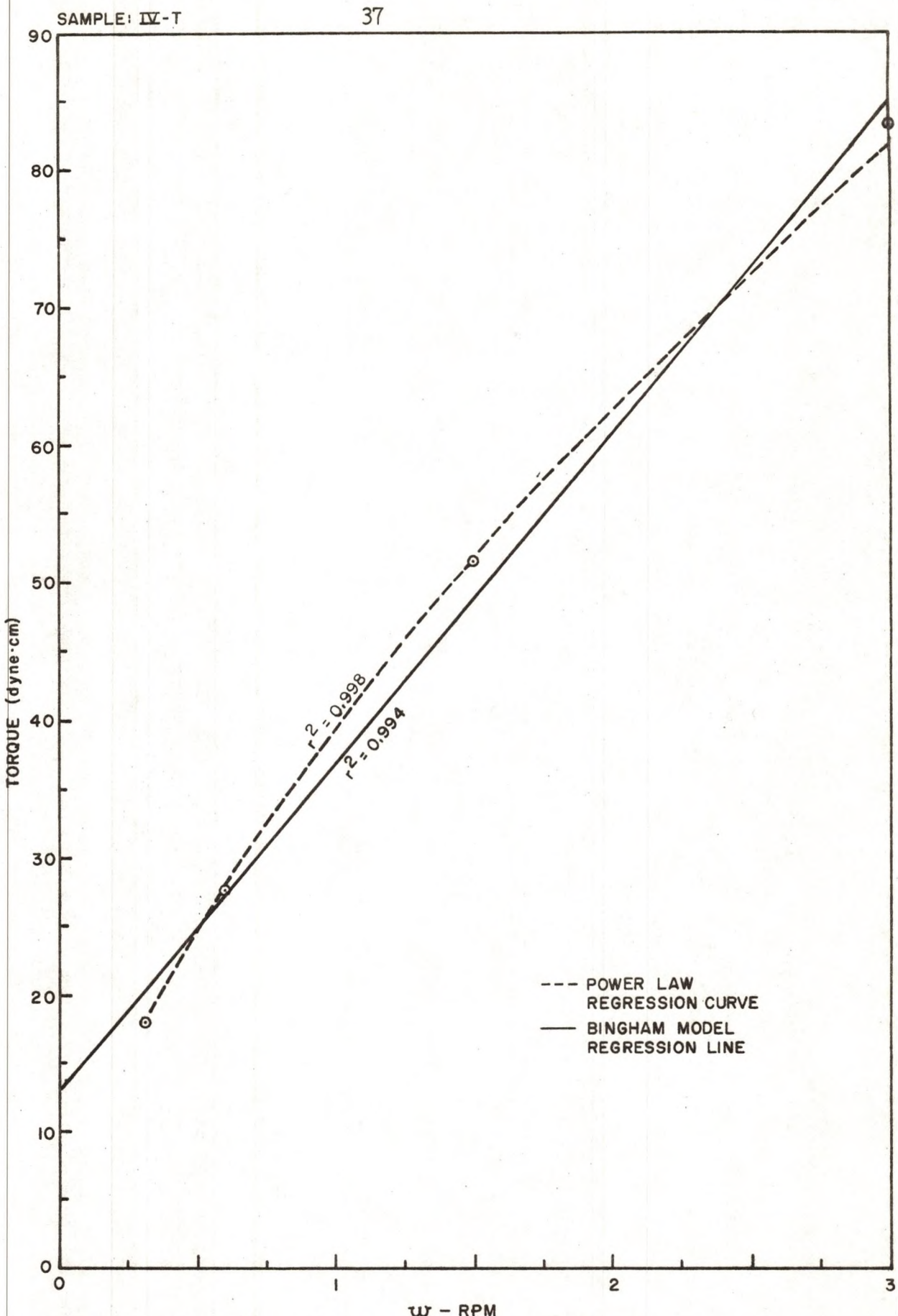

FIGURE 14 - TORQUE VERSUS ANGULAR VELOCITY AT 350° F

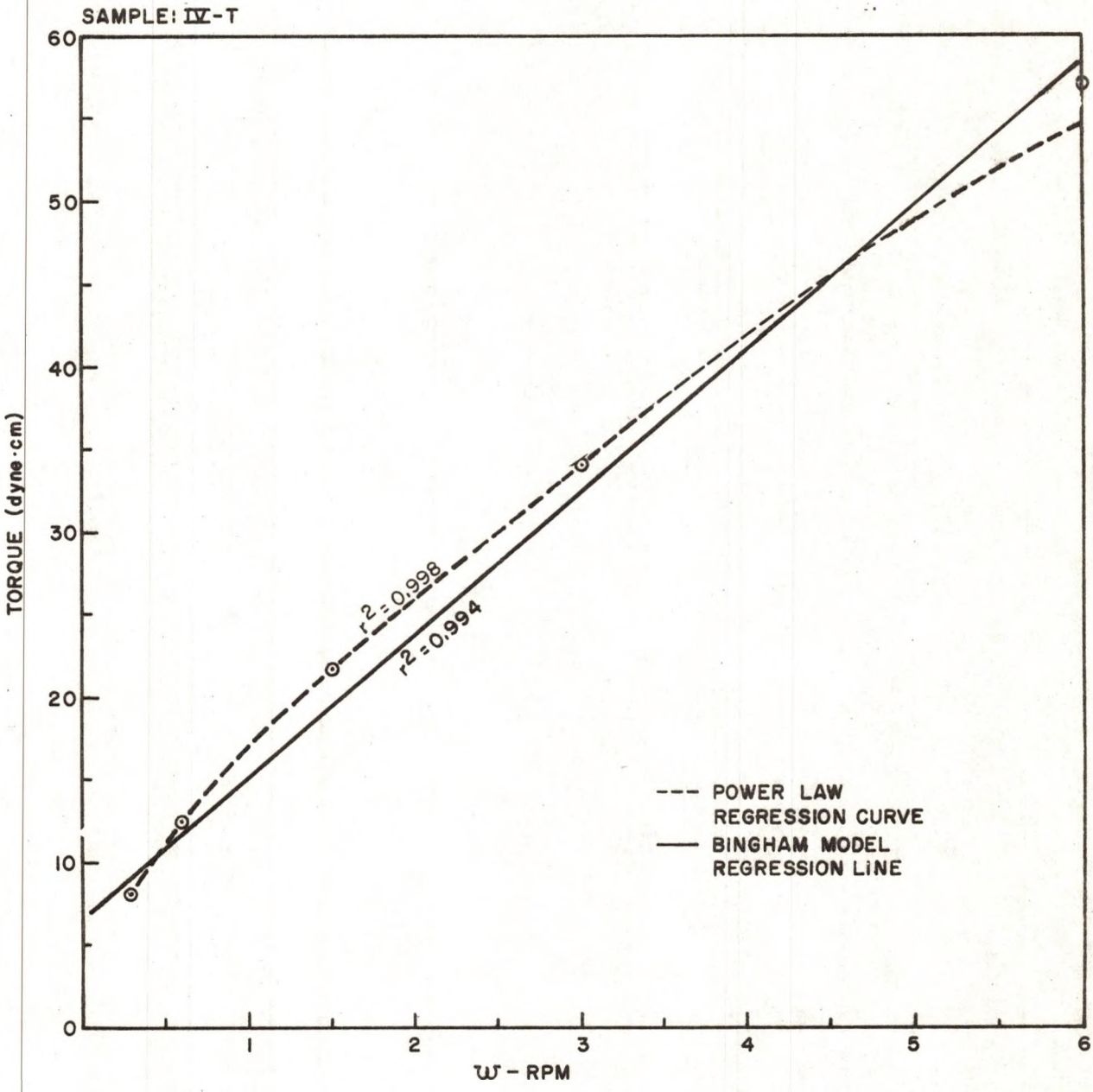

FIGURE 15- TORQUE VERSUS ANGULAR VELOCITY RELATIONSHIP AT 375° F

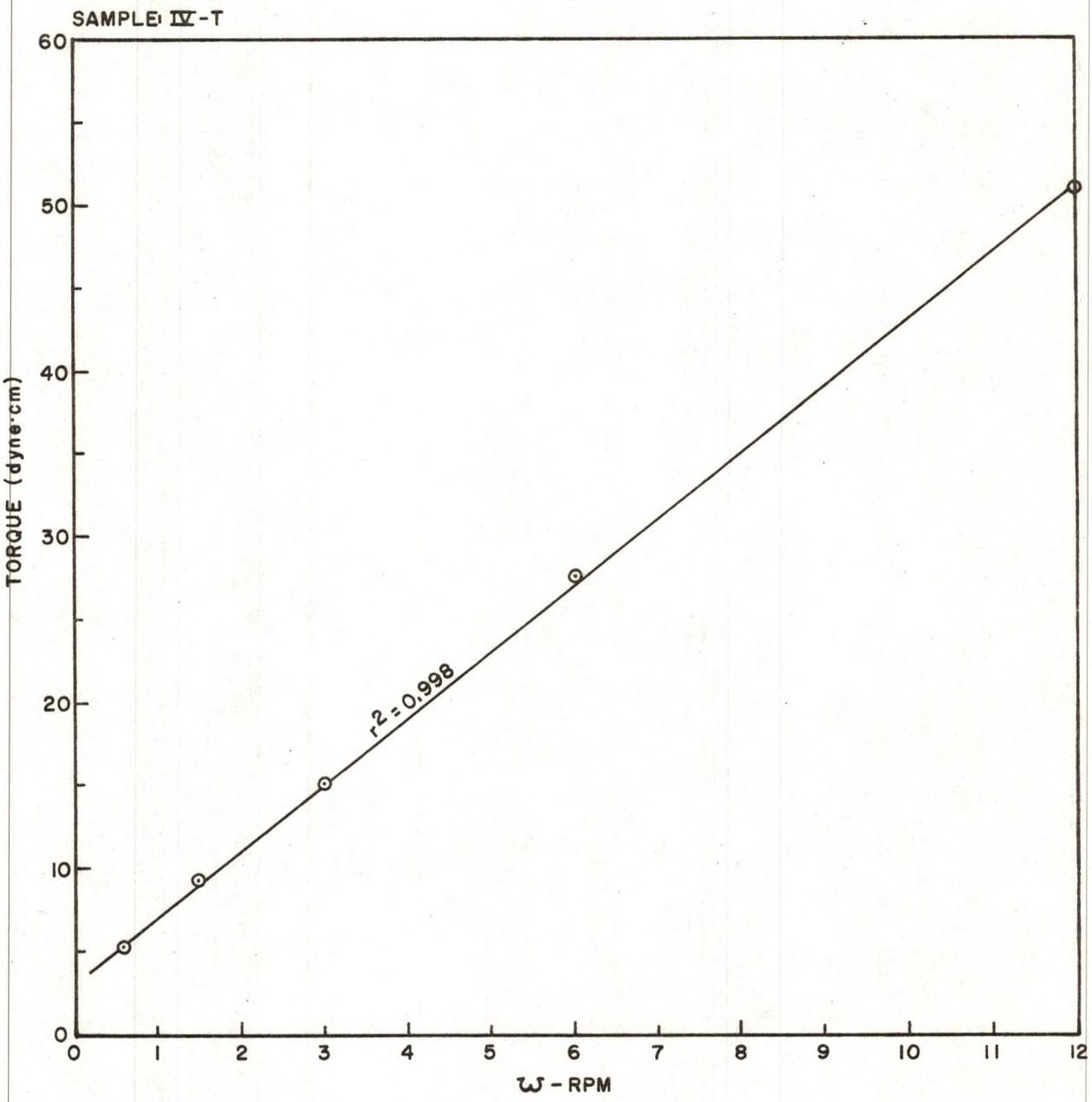

FIGURE 16 - TORQUE VERSUS ANGULAR VELOCITY RELATIONSHIP AT 400° F

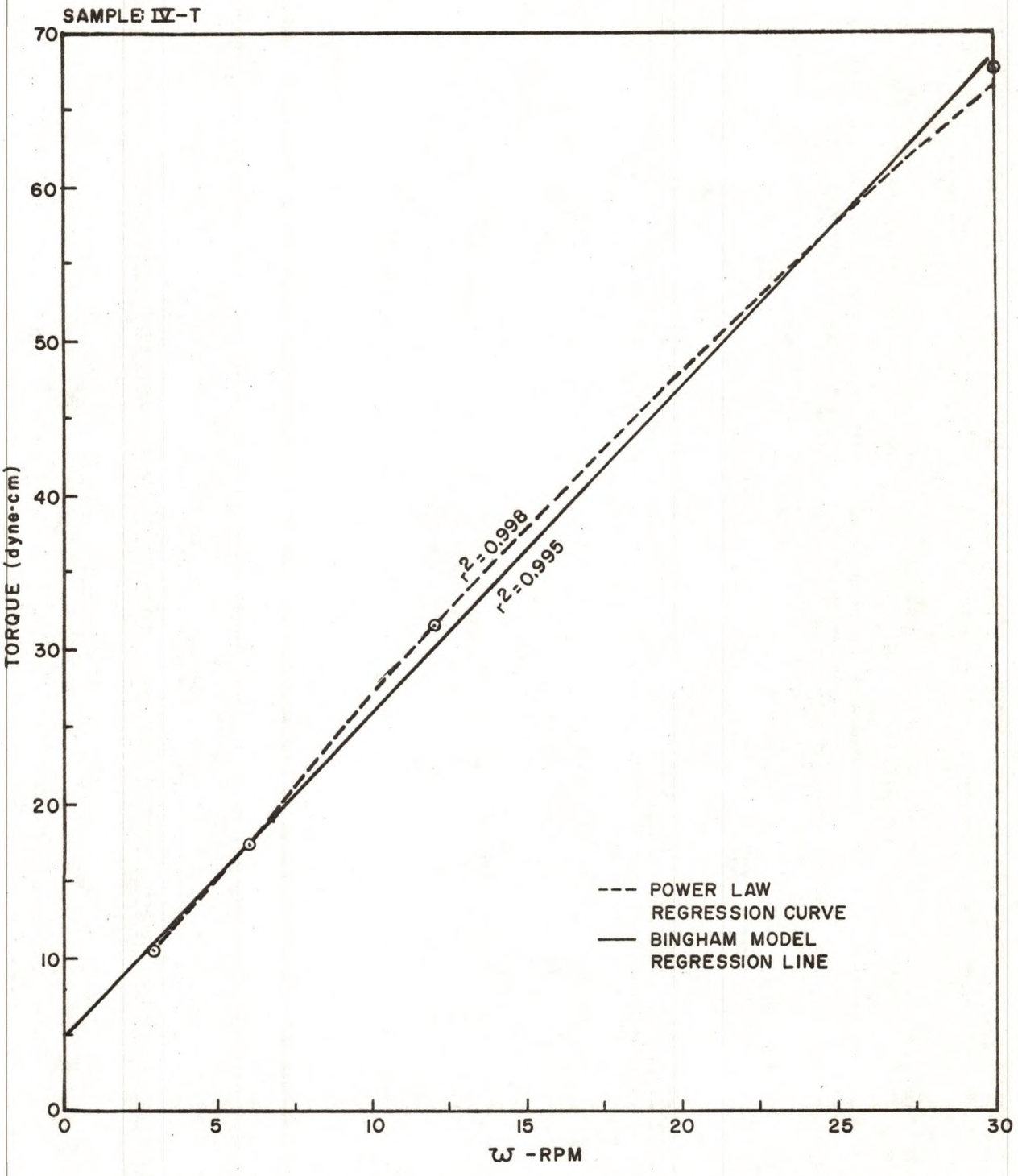

FIGURE 17 - TORQUE VERSUS ANGULAR VELOCITY RELATIONSHIP AT 425° F

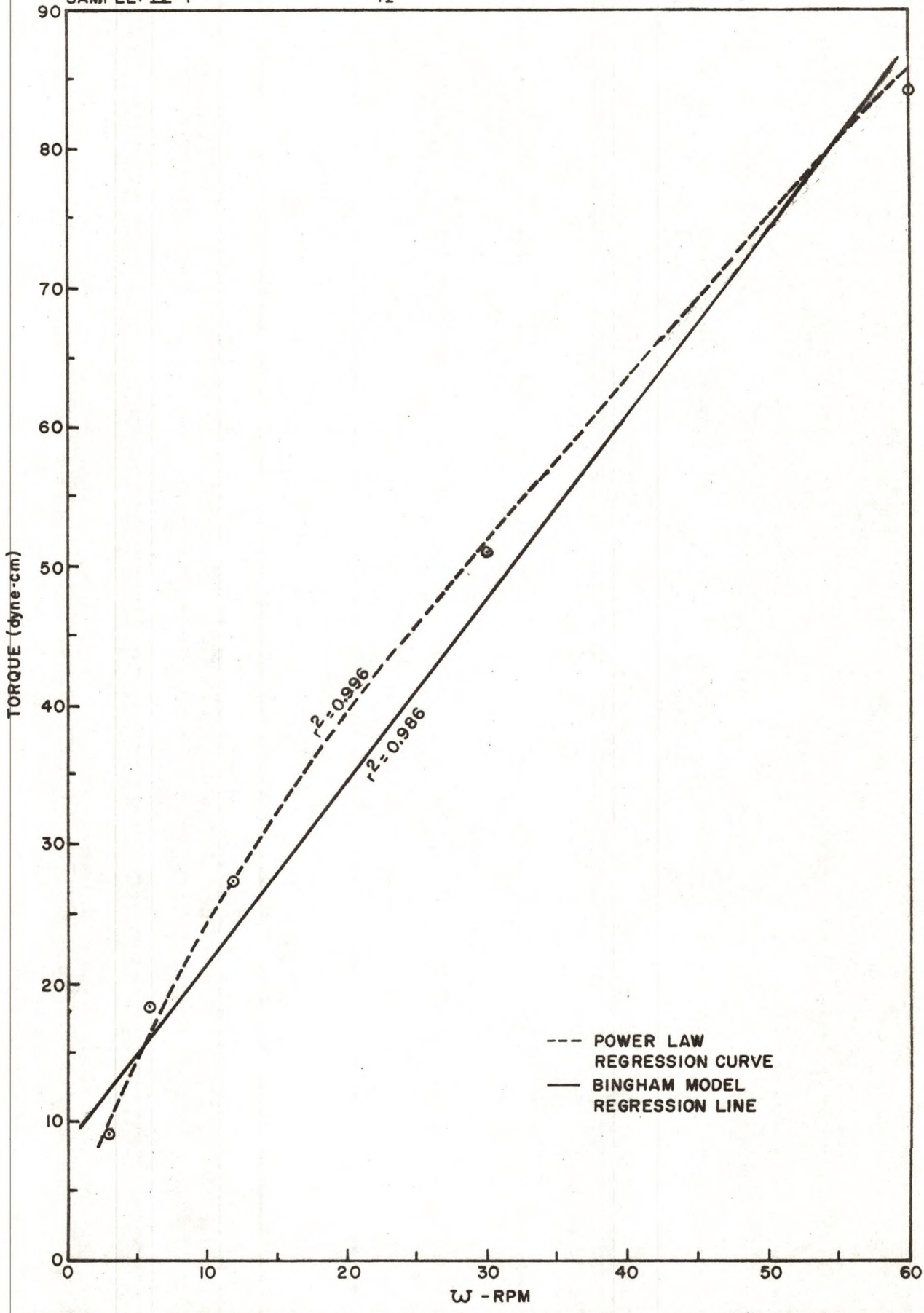

FIGURE 18 - TORQUE VERSUS ANGULAR VELOCITY RELATIONSHIP AT 450° F

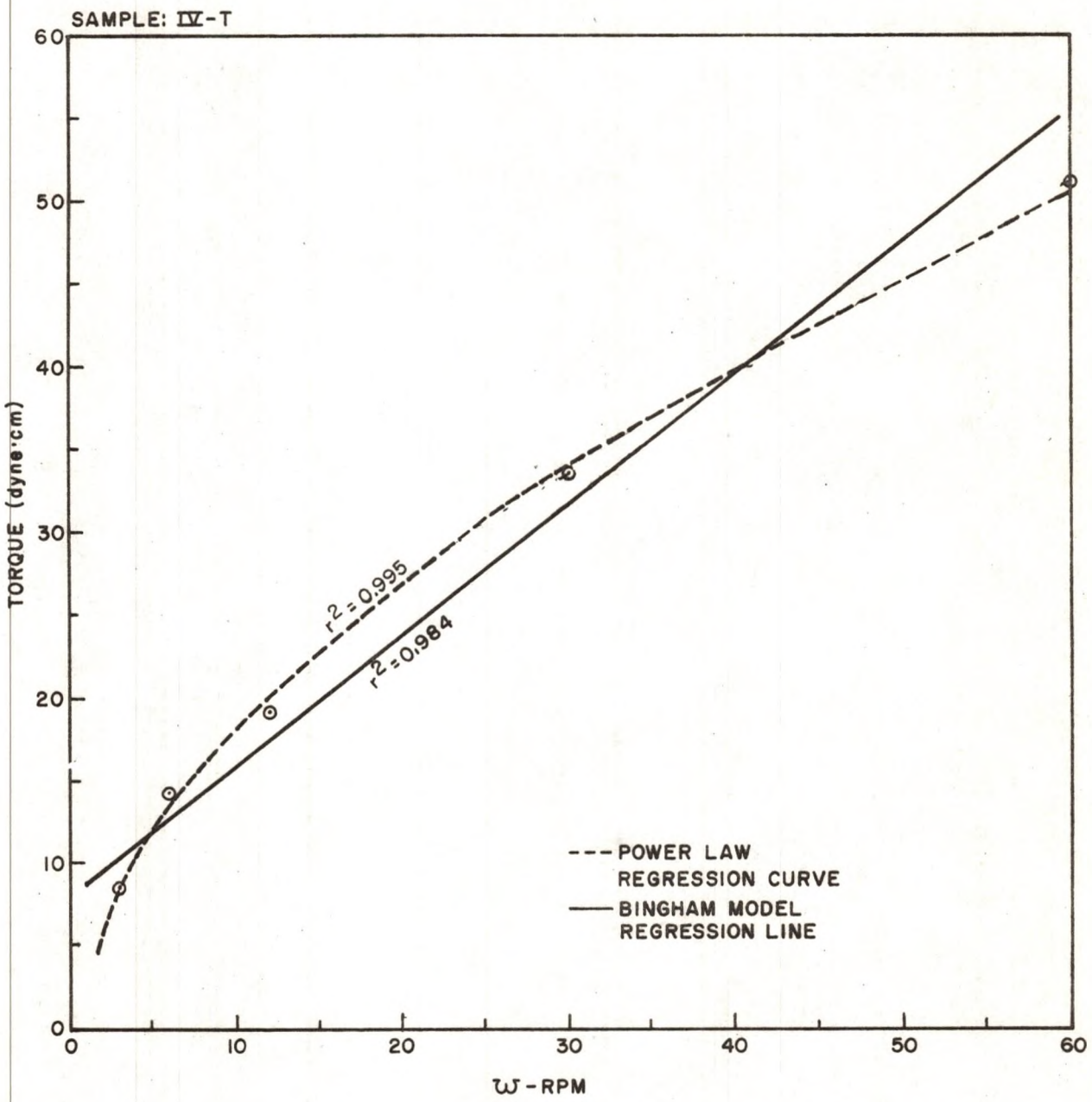

FIGURE 19 - TORQUE VERSUS ANGULAR VELOCITY RELATIONSHIP AT 475° F

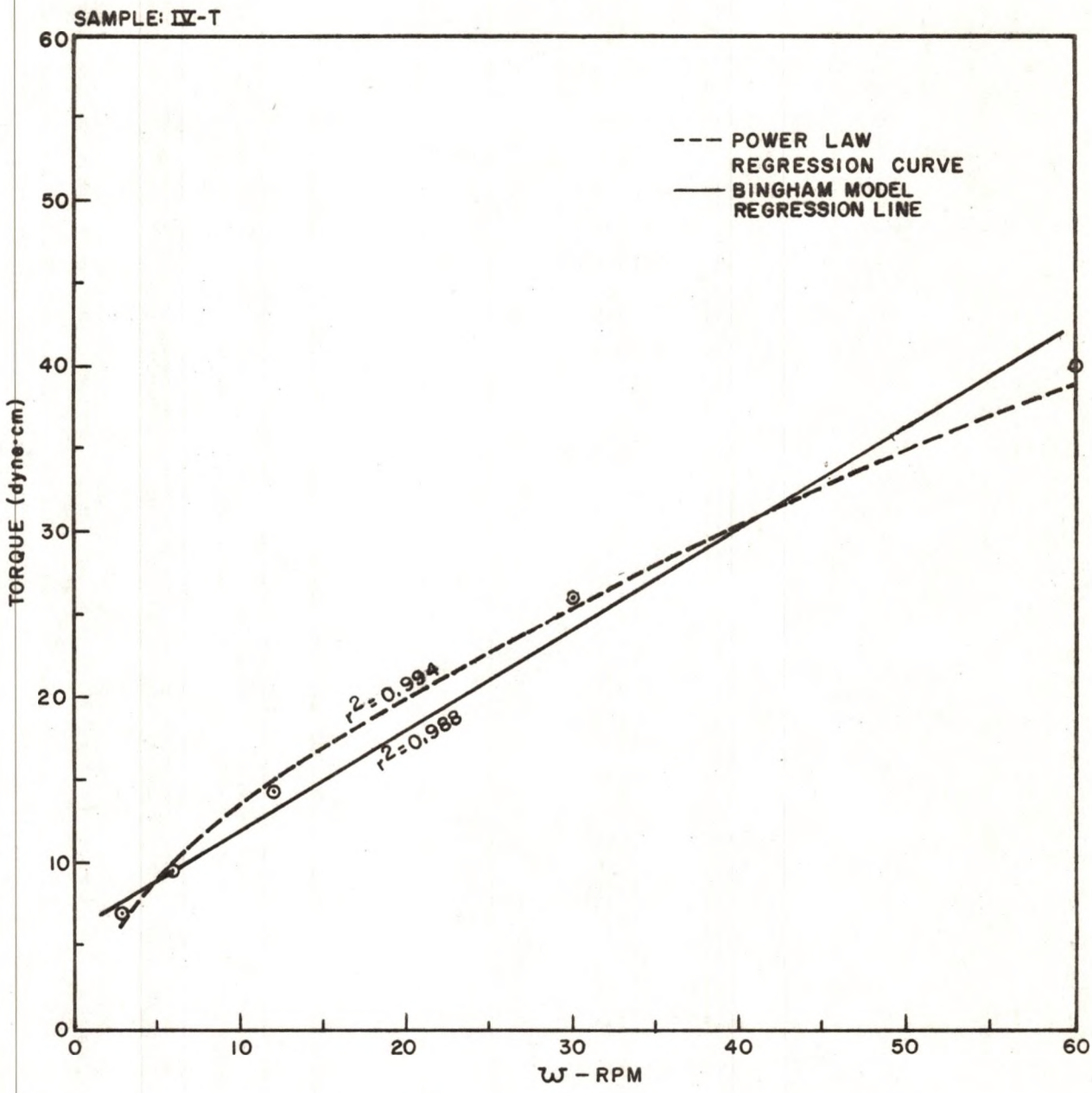

FIGURE 20- TORQUE VERSUS ANGULAR VELOCITY RELATIONSHIP AT 500° F

were made at intervals of 25 degrees. To avoid hysteresis effects due to temperature, the measurements were made in ascending order of temperature only. The regression lines for both models have been drawn on the plot. At all temperatures the power law model consistently fits the data closer than the Bingham model. Deviations from the Bingham model increase as the temperature increases.

3. Effect of Temperature on Power Law Model Parameters

Figures 21 and 22 show the relation of the power law parameters 'n' and 'm' with temperature respectively. It can be seen from Figure 21 that 'n' increases first as temperature is increased until 425^{o}F, and then starts to decrease. The parameter 'm', on the other hand decreases monotonically with increase of temperature.

4. Effect of SRL Melting Point and Ash Content on Power Law Exponent 'n'

Figure 23 is a plot of 'n' versus the melting point and ash content for samples from group III. The values of 'n' were calculated using the method of Appendix I. It can be seen that 'n' relates linearly with melting point of SRL, whereas it relates to the ash content by a power greater than one.

Effect of Process Variables and Sample Properties of SRL Apparent Viscosity.

In this section, correlations were made between the apparent viscosity of SRL and temperature of sample measurement, and with process variables of the liquefaction process such as solvent to coal ratio of the feed, degree of conversion (of the original

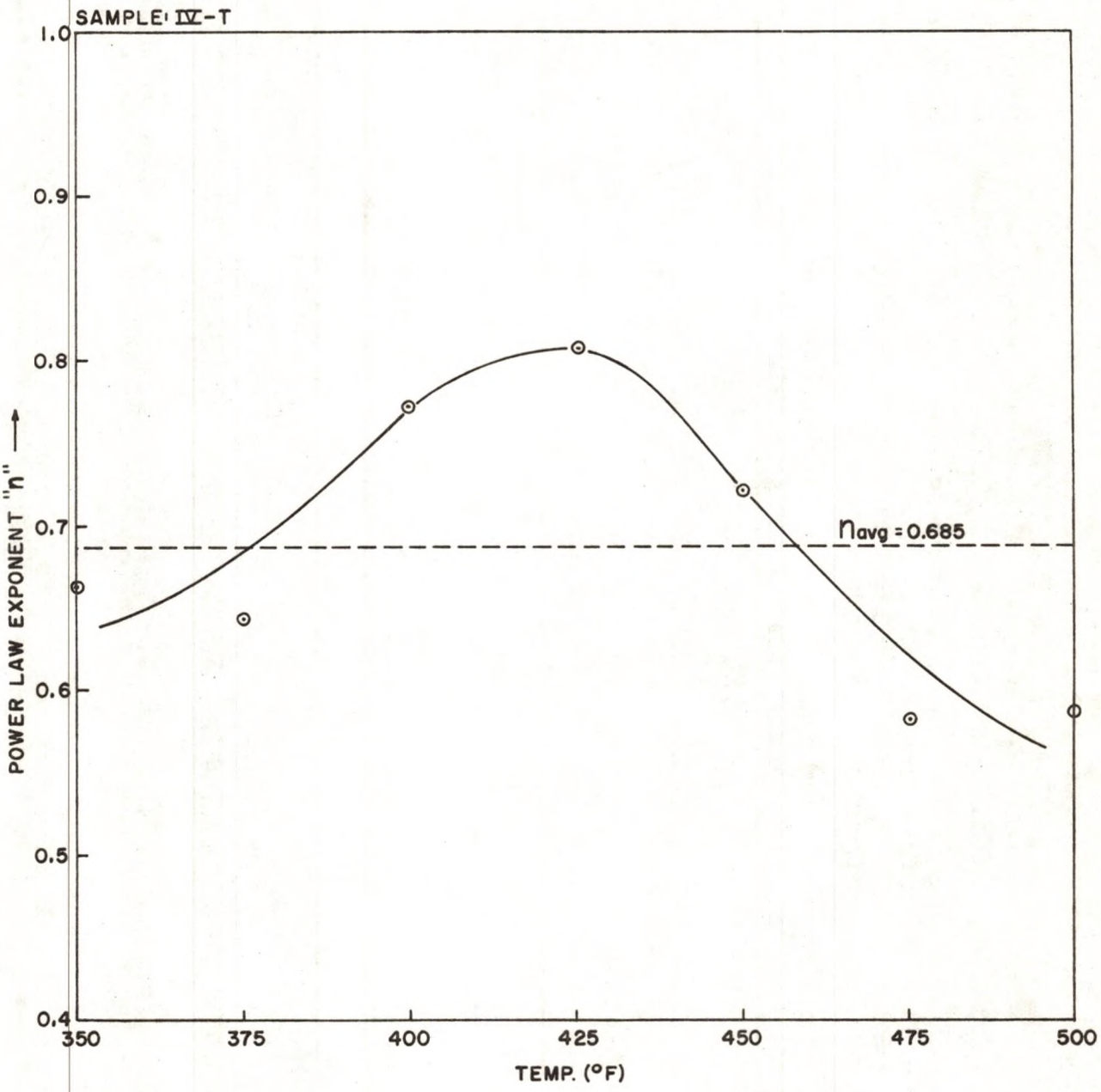

FIGURE 21- EFFECT OF TEMPERATURE ON POWERLAW EXPONENT "n"

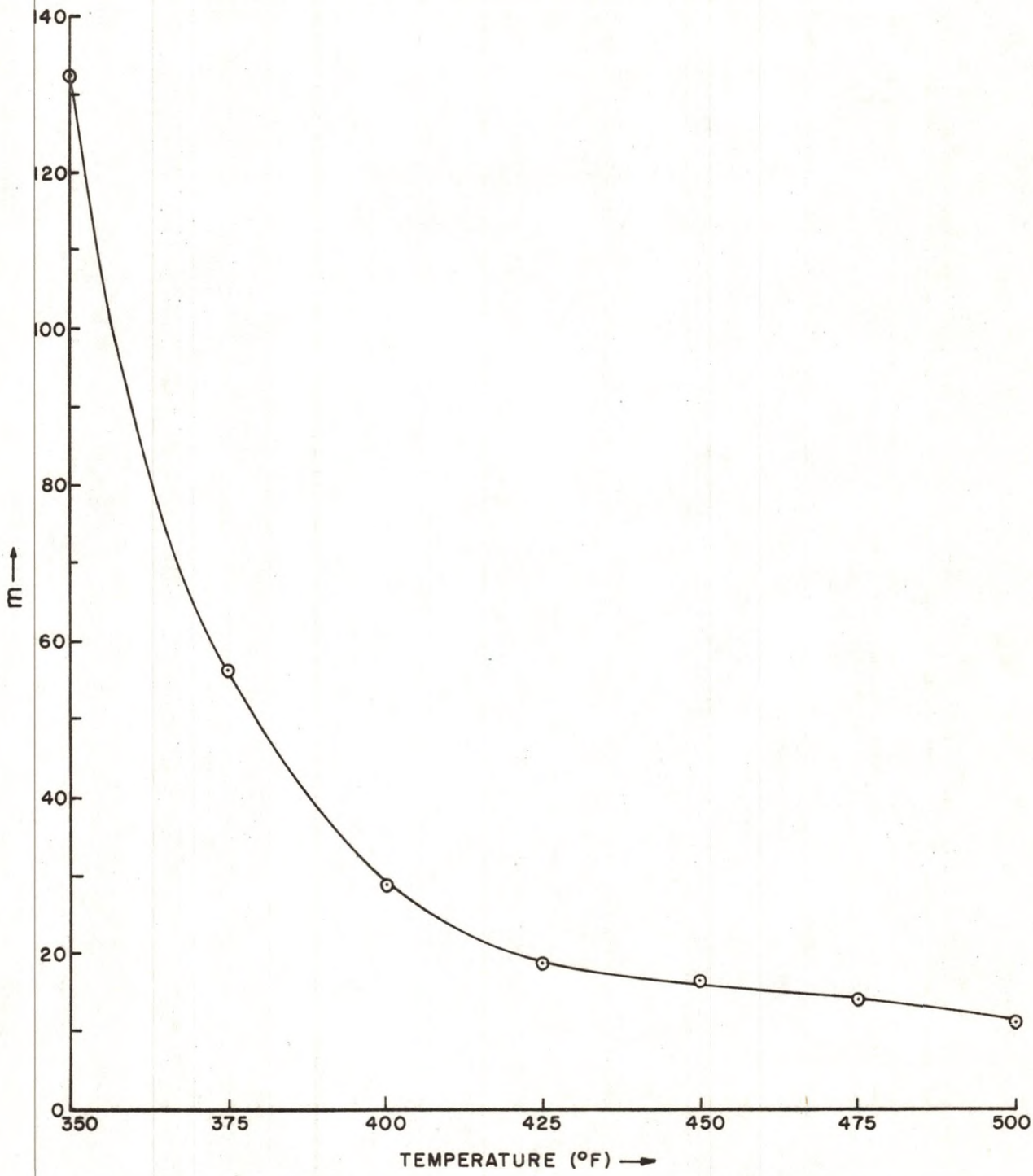

FIGURE 22-EFFECT OF TEMPERATURE ON POWER LAW COEFFICIENT "m"

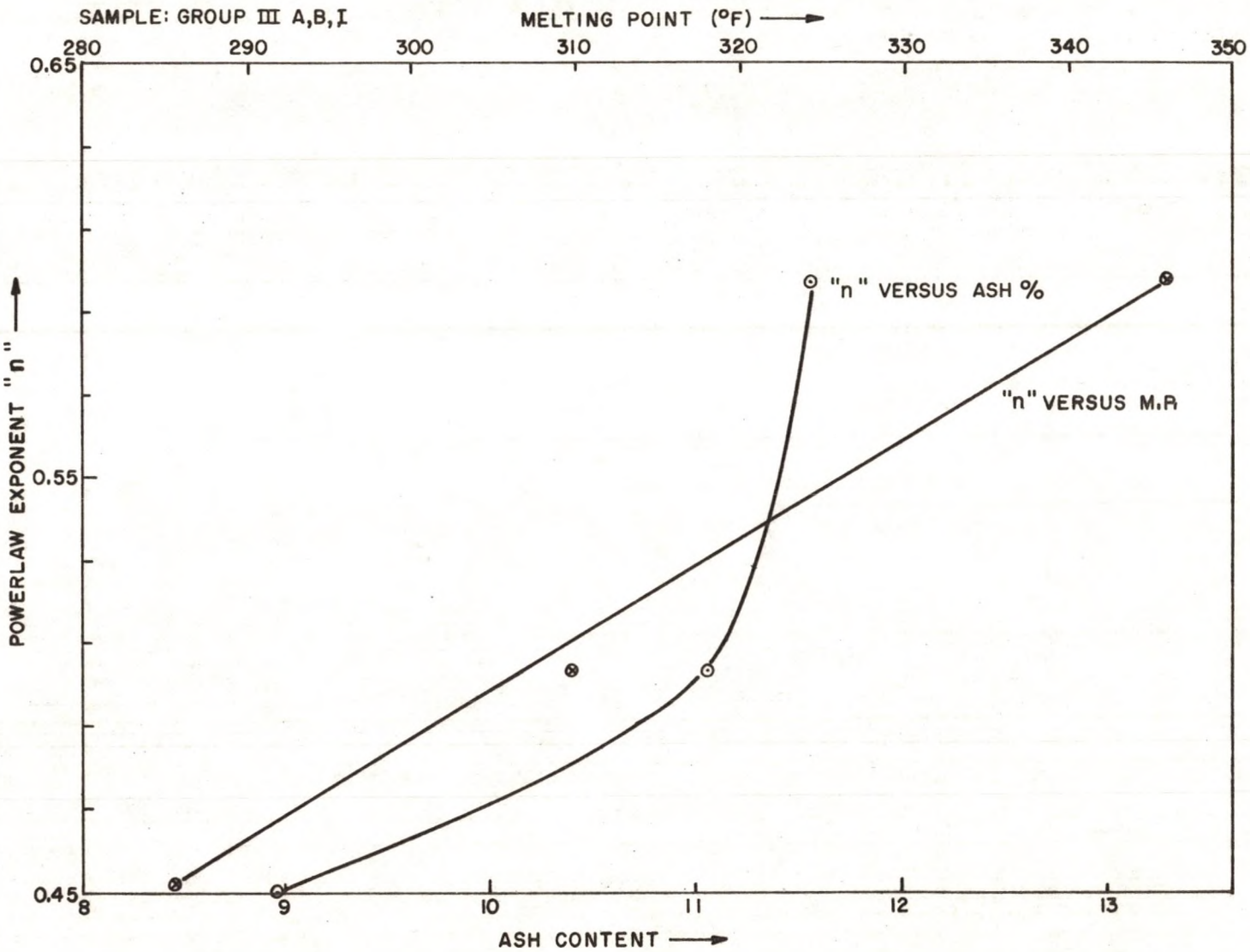

FIGURE 23 - VARIATION OF POWERLAW EXPONENT "n" WITH ASH CONTENT AND MELTING POINT

moisture free lignite to SRL). Apparent viscosity was also related to sample properties such as ash concentration, solvent weight content, molecular weight average, and density.

Among the process variables studied, the degree of conversion and solvent to coal ratio of feed did not show any definite correlation with the apparent viscosity of the SRL. Temperature did however affect the apparent viscosity of SRL, and is discussed in detail below.

1. Effect of Temperature on SRL Apparent Viscosity

Figures 24 and 25 show the variation of the viscosity of sample IV-T with measurement temperature. In Figure 24 the apparent viscosity data are presented at 3 rpm and in Figure 25, at 6 rpm. Both plots show an approximately exponential decrease of the viscosity with an increase of temperature. Figure 26 is a semi-log plot of apparent viscosity of the sample against the reciprocal of the temperature, at angular velocities of 3, 6 and 12 rpm. The data are seen to approximate a straight line. It can also be observed that apparent viscosities measured at higher angular velocities give better correlation with temperature. This is explained by the fact that at higher speeds there is better mixing of the sample which reduces the temperature gradients and gives a more uniform temperature throughout the sample.

The relation of apparent viscosity of SRL to temperature can be expressed mathematically as follows.

$$\mu = A \times T^{-B} \quad \ldots\ldots\ldots\ldots\ldots\ldots\ldots\ldots\ldots\ldots \quad (7.1)$$

where A and B are non-negative constants,

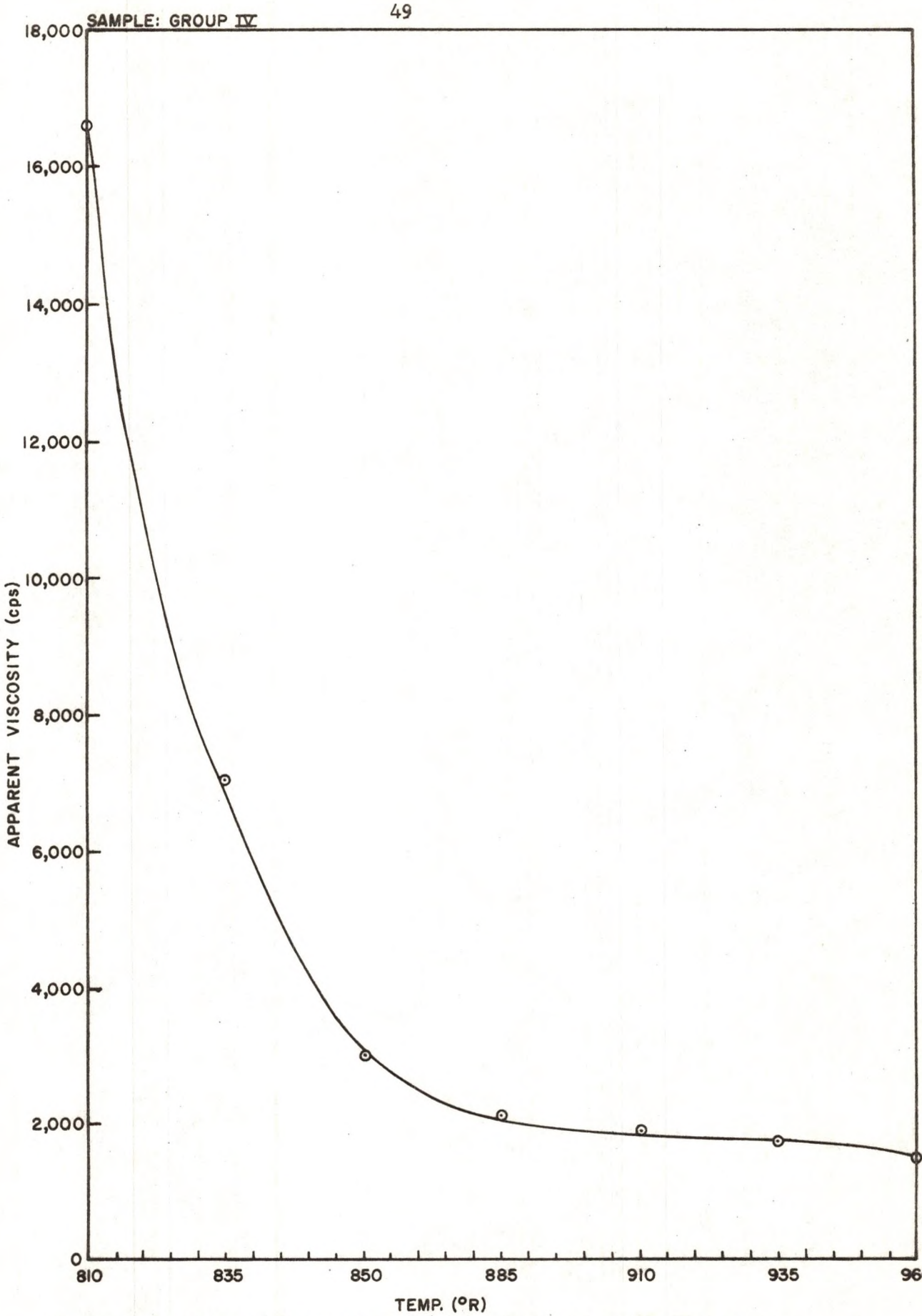

FIGURE 24-APPARENT VISCOSITY VERSUS TEMPERATURE

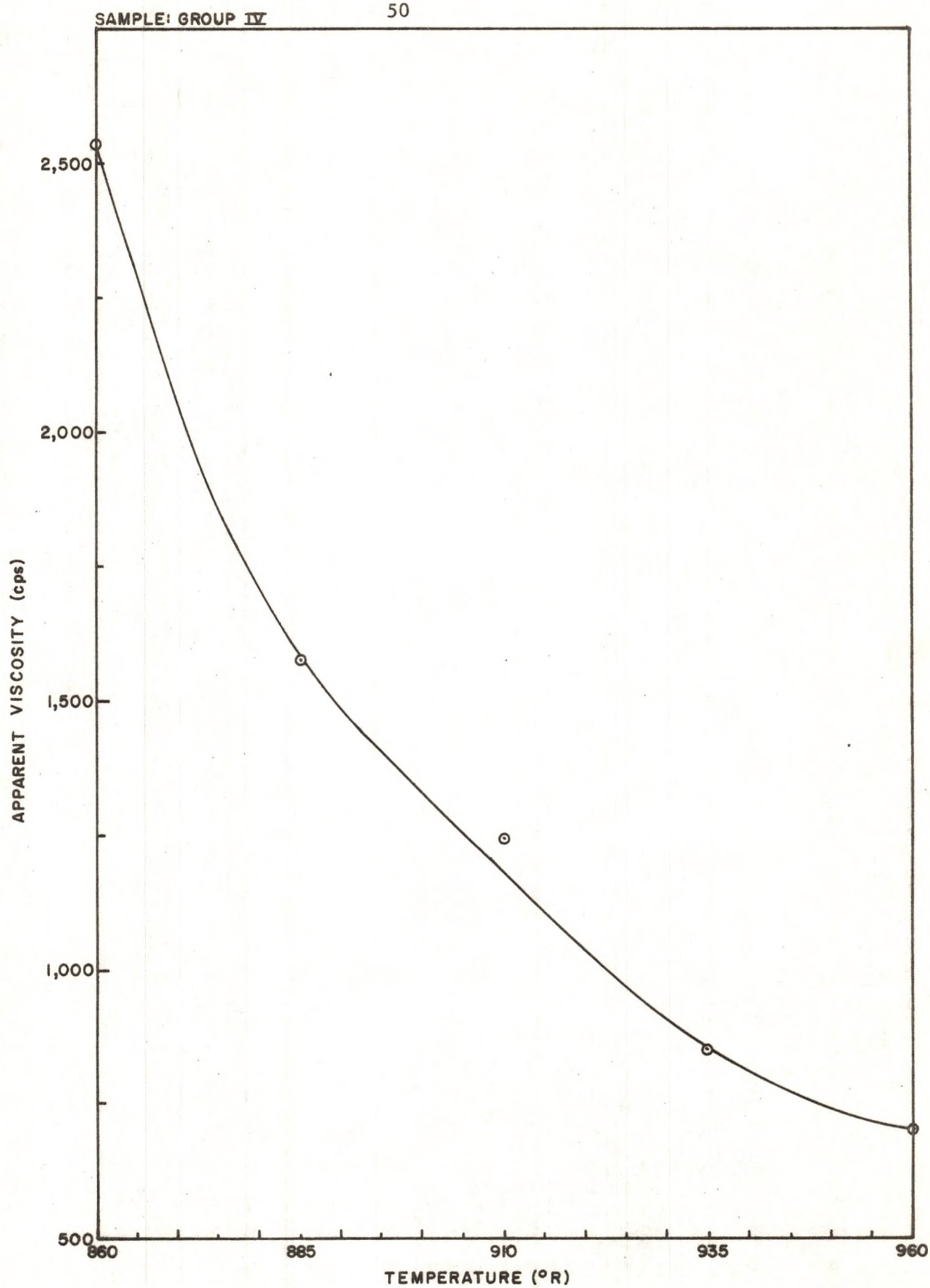

FIGURE 25 - APPARENT VISCOSITY VERSUS TEMPERATURE

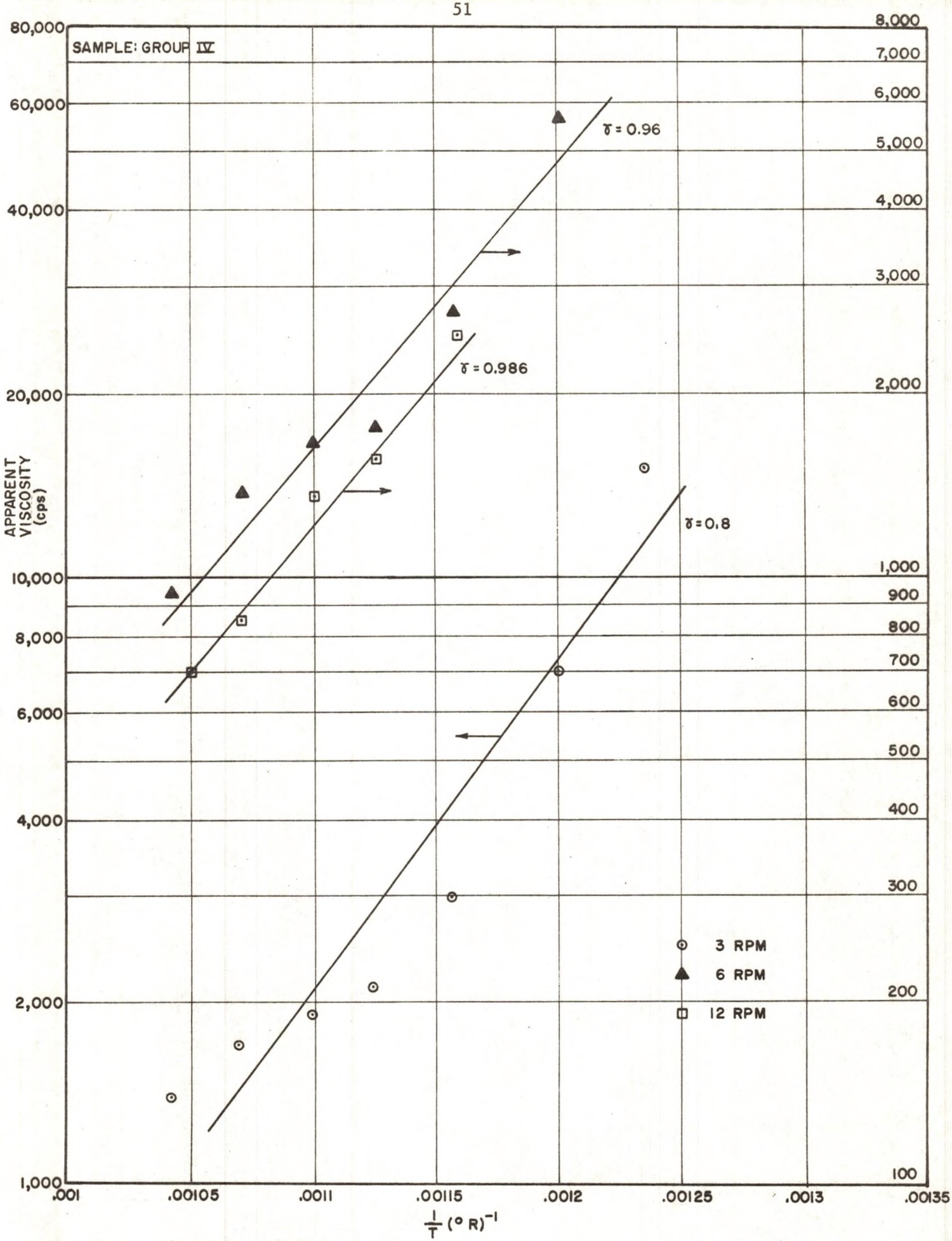

FIGURE 26- EFFECT OF TEMPERATURE ON VISCOSITY

T is the absolute temperature in ^{o}R

μ is the apparent viscosity in centipoises.

Calculated values for the constants in Figure 26 are given below.

TABLE 2

CONSTANTS IN THE APPARENT VISCOSITY-TEMPERATURE RELATIONSHIP

Speed of rotation of spindle	A	B
3 rpm	-2.0	4640
6 rpm	-1.7	4470
12 rpm	-1.6	4400

2. Effect of Sample Melting Point on SRL Apparent Viscosity

Figure 27 shows the relationship between melting point and apparent viscosity of six samples from group III, at three different angular velocities. Data closely fit a straight line. It can also be seen that better fit results at higher angular velocities.

An empirical relation of the following form can be proposed for the melting point apparent viscosity relationship.

$$\mu = A + B \times M \qquad (7.2)$$

where μ is the apparent viscosity in centipoises,

M is the melting point in deg F,

A & B are non-negative constants.

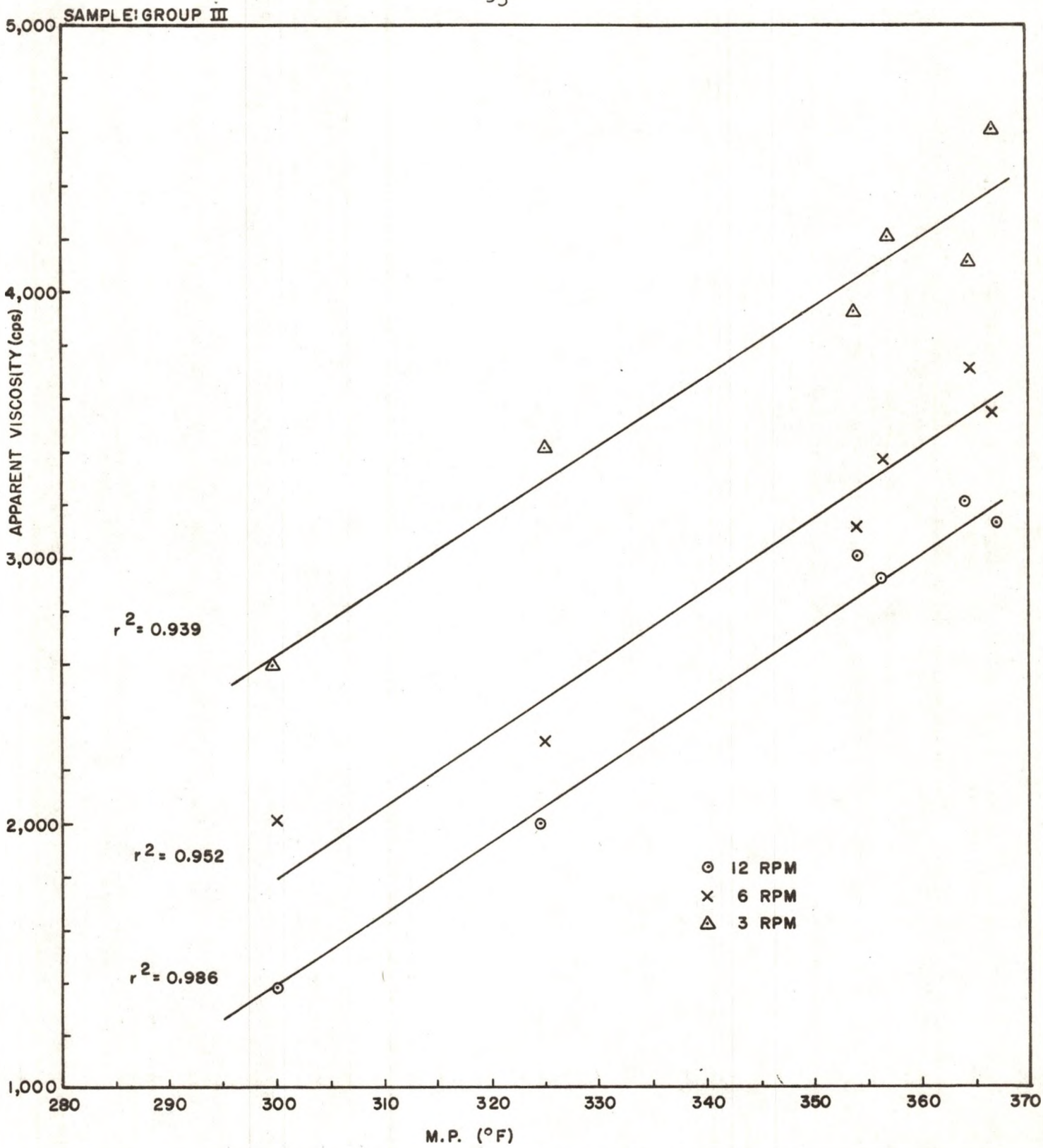

FIGURE 27 - MELTING POINT VERSUS APPARENT VISCOSITY

Values of the constants A and B obtained from Figure 28 are listed below.

TABLE 3

CONSTANTS IN THE APPARENT VISCOSITY-MELTING POINT RELATIONSHIP

Speed of rotation	A	B
3 rpm	-5090	25.8
6 rpm	-5790	25.5
12 rpm	-7800	30.1

Figure 28 shows the variation of SRL melting point and apparent viscosity as a function of time during a PDU run. Spot samples were taken at random intervals and viscosities and melting points determined. The melting point versus time plot and the apparent viscosity versus time plot are similar indicating that samples apparent viscosity correlates roughly with its melting point. The sample melting point is in turn dependent on factors such as the solvent content, ash content, asphaltene content and the composition of the other organic compounds which make up the sample. It is of interest therefore to study the effect of these factors on the apparent viscosity of the sample.

3. Variation of SRL Apparent Viscosity with Ash Concentration

Figure 29 is a semi-log plot of the ash content versus the apparent viscosity of samples of group III. The straight line relationship on this plot indicates that ash content bears an exponential relationship with apparent viscosity. This relationship

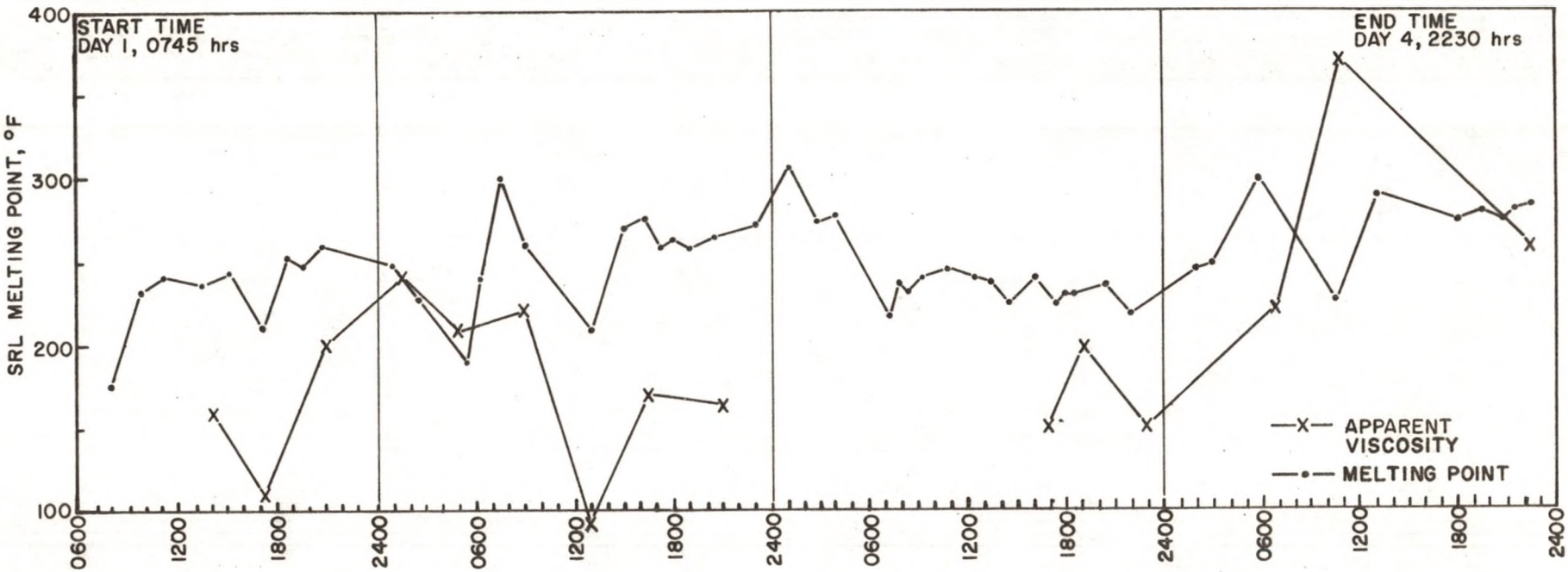

FIGURE 28 - VARIATION OF APPARENT VISCOSITY AND MELTING POINT WITH RUNTIME

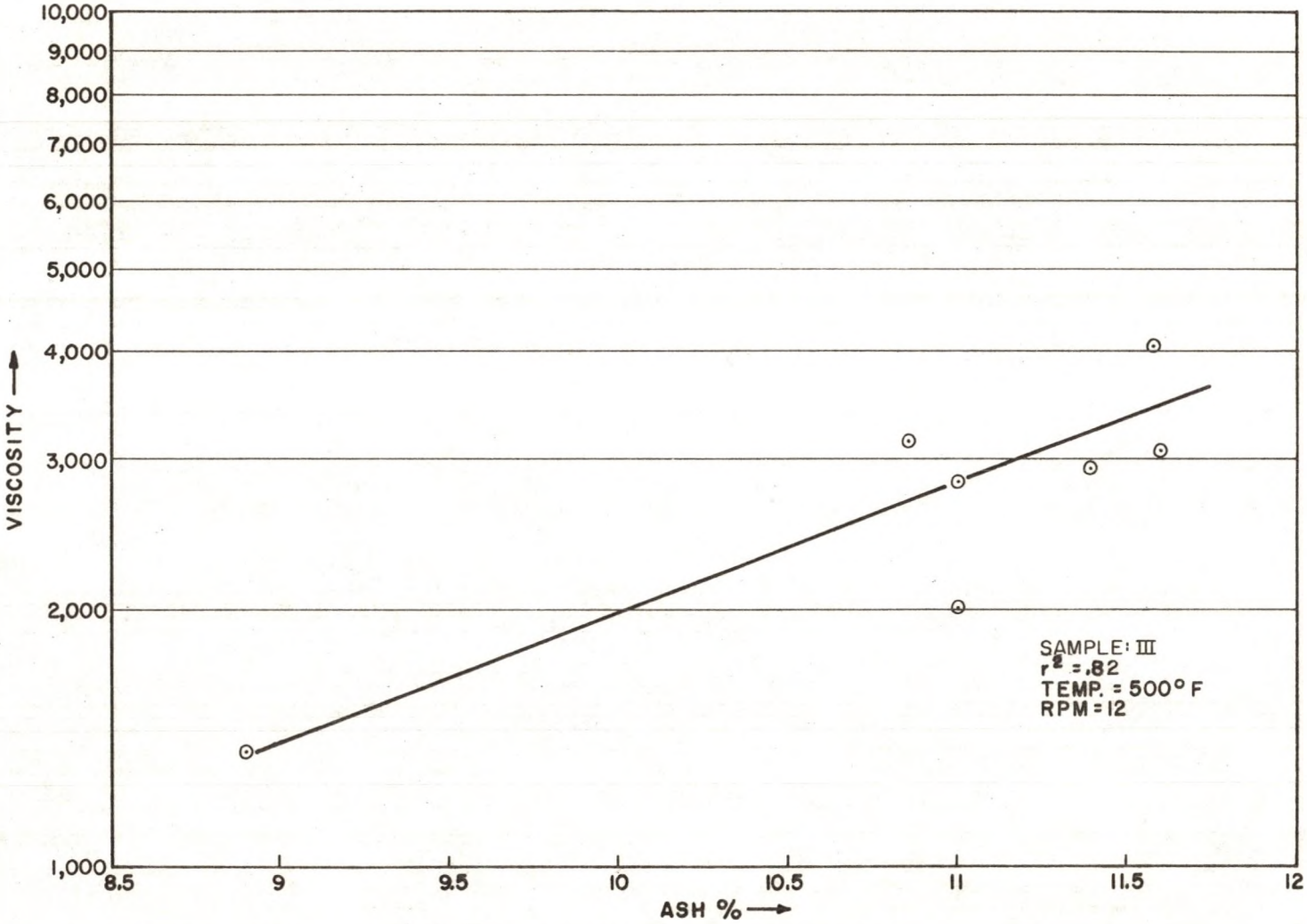

FIGURE 29 - VISCOSITY VERSUS ASH CONTENT

can be expressed mathematically as

$$\mu = A \times B^{W} \qquad (7.3)$$

where μ is the apparent viscosity in centipoises,

W is the ash concentration by weight,

A & B are non-negative constants.

Effect of sample density (solid) on the apparent viscosity was also investigated. No definite correlation was found between SRL apparent viscosity and its solid density.

4. Variation of SRL Apparent Viscosity with Average Molecular Weight*

Figure 30 shows the relationship between the apparent viscosity of SRL and the average molecular weight of the THF soluble portion of the SRL sample. The plot shows an exponential increase in apparent viscosity with an increase in the average molecular weight. This indicates that the larger and heavier molecules contribute to increasing the apparent viscosity by greater amounts than the lighter molecules. This is understandable because viscosity is defined as a measure of the internal friction of a fluid, and the presence of heavier molecules causes more friction in the movement of the fluid layers, resulting in increased viscosity. Details of the molecular weight determination average are presented in Appendix C.

5. Effect of Solvent Content of SRL Sample on its Apparent Viscosity

Figures 31, 32 and 33 show the variation of SRL apparent

*Indicates the molecular weight average of the tetra-hydro furan (THF) soluble portion of the sample as determined by GPLC.

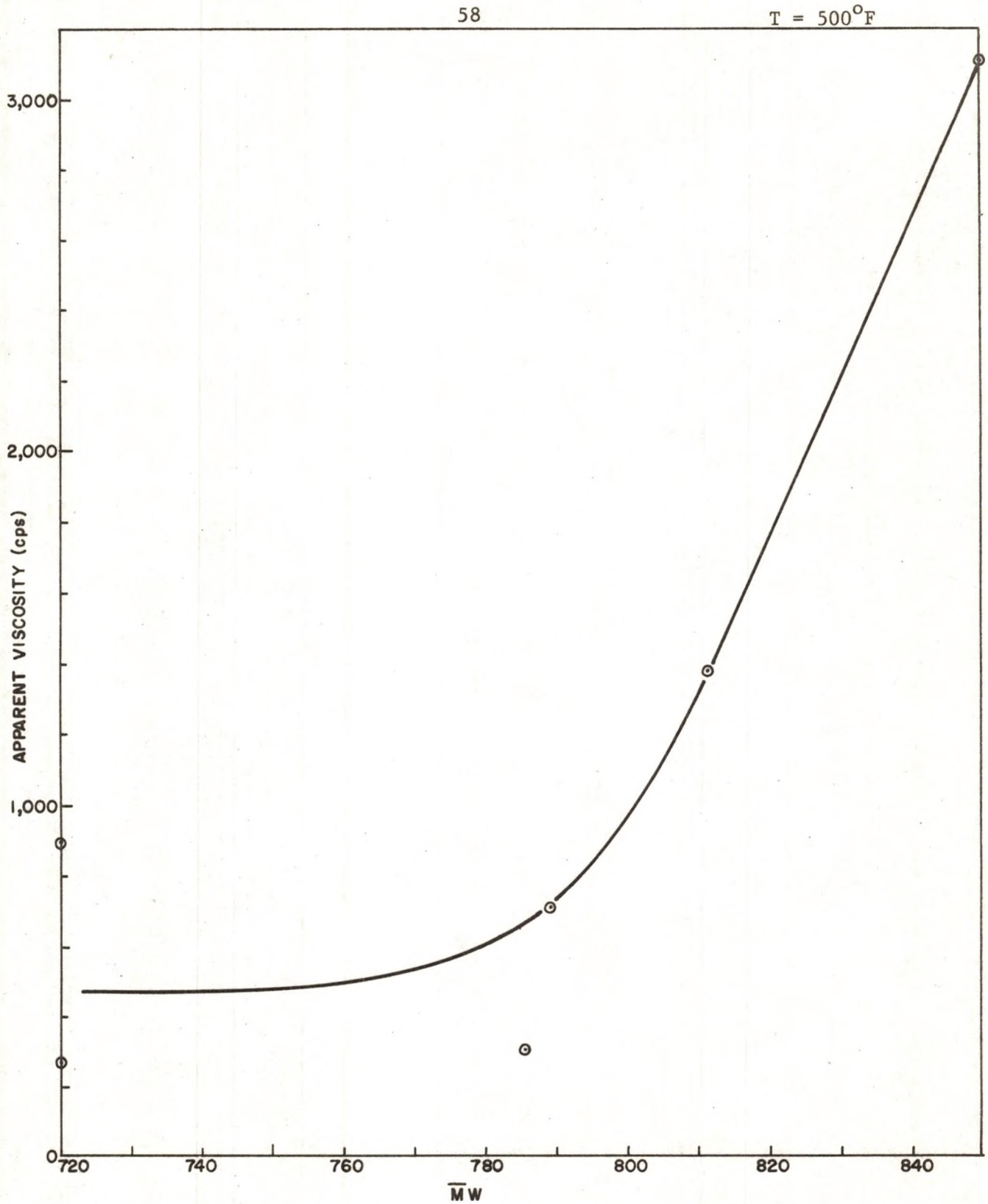

FIGURE 30- APPARENT VISCOSITY VERSUS MOL·WT AVERAGE OF THF SOLUBLES ($\overline{M}W$)

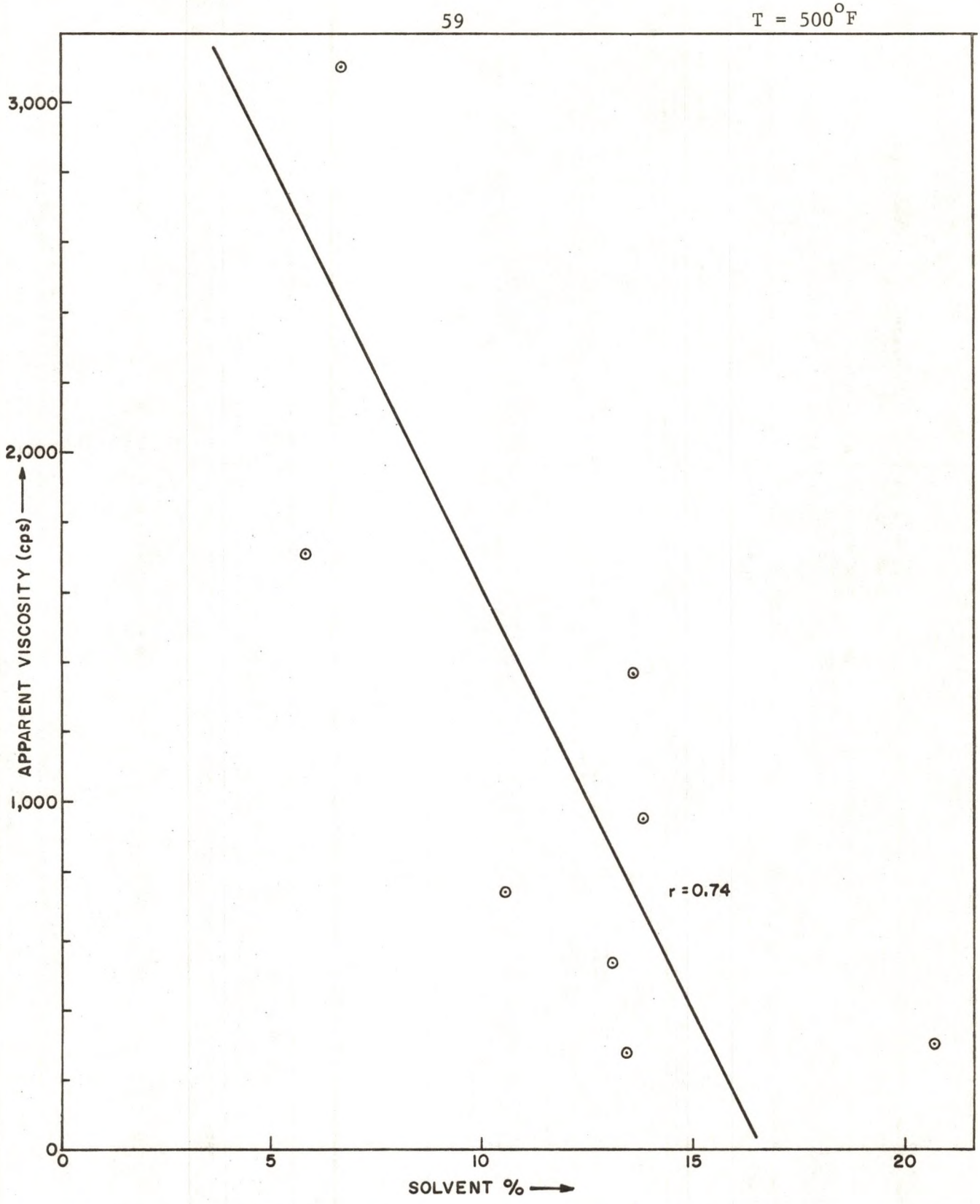

FIGURE 31 - APPARENT VISCOSITY VERSUS SOLVENT % (By Micro Distillation)

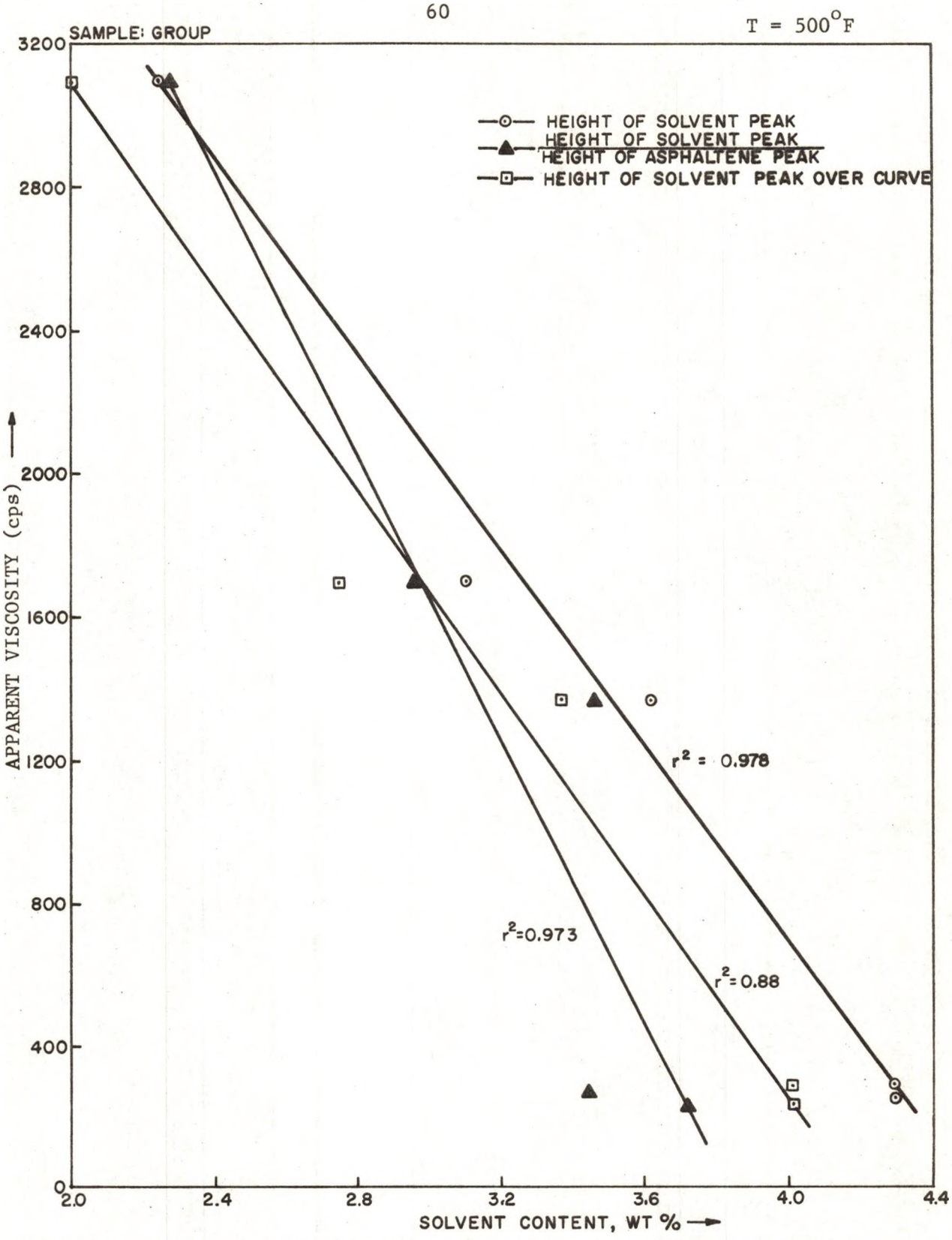

FIGURE 32 - APPARENT VISCOSITY VERSUS SOLVENT CONTENT
(Calculated From GPLC Data)

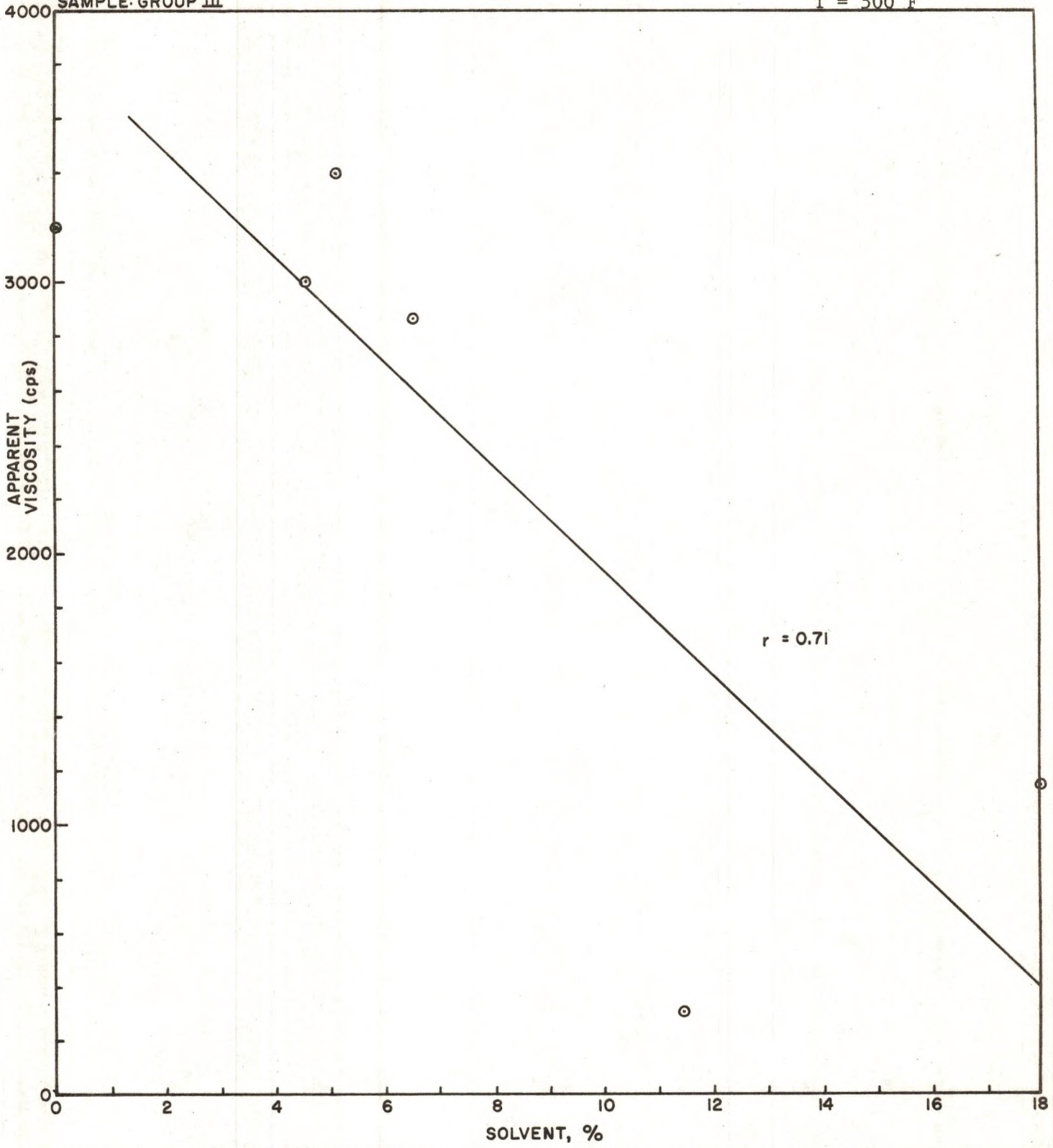

FIGURE 33 - APPARENT VISCOSITY (cps) VERSUS SOLVENT % BY WEIGHT (Calculated)

viscosity with the solvent content of the sample. In each of these plots the solvent content was calculated by a different method.

In Figure 31 the solvent content was obtained from micro-distillation measurements performed by the Grand Forks Energy Research center. Details of this measurement are given in Appendix C. As the figure shows the solvent content relates linearly with the apparent viscosity at correlation coefficient of 0.74.

Figure 32 shows the relation between apparent viscosity of SRL and its solvent content calculated from Gel Permeation Liquid Chromatography (GPLC) measurements done at the Grand Forks Energy Research Center.

Figures 34 and 35 in Appendix C are the result of this measurement. SRL apparent viscosity is found to relate linearly with the solvent contents calculated by this method.

Figure 33 shows the relation between SRL apparent viscosity and its solvent content calculated by material balances. These calculations are given in detail in Appendix C. In this case also a linear relation was observed between SRL apparent viscosity and its solvent content.

These plots thus show that viscosity of SRL decreases linearly with increase in its solvent content.

6. Combined Effect of the Chemical Constituents of SRL on the Apparent Viscosity

1. It was shown earlier that SRL melting point was linearly related to its viscosity. It was therefore decided to investigate the combined effect of solvent content, ash content and various

other organic compounds on the apparent viscosity of SRL. The organic compounds considered were aliphatics, ethers, compounds with nitrogen and oxy acids. The percentages of these compounds in the SRL samples were calculated from GPLC measurements done at the Grand Forks Energy Research Center. Appendix C gives the complete data of the tests done at the Grand Forks Research Center.

Multiple linear correlation was done between the SRL apparent viscosity and the following variables in composition: 1) Solvent content 2) Ash concentration 3) Aliphatics content 4) Ethers content 5) Nitrogen compounds content and 6) Oxy acids content. The initial analysis gave a correlation coefficient 'r^2' of 0.97. The term or terms least affecting the regression equation were then dropped. The basis for selecting which term to drop was the "t" value from the student "t" test. A new regression equation was then developed with the remaining variables, and this process was repeated until finally a regression equation was obtained with only three variables from the original six remaining. These three variables were found to significantly affect the regression equation and the elimination of any of these variables was found to lower the correlation coefficient significantly. The table below is the summary of the results. The final equation obtained was found to explain 93 percent of the data with only three variables. The number of data points used in this analysis was eight. The three variables most significantly affecting the apparent viscosity of SRL were solvent content, percent aliphatics and percent ethers.

TABLE 4

RESULTS OF MULTIPLE LINEAR CORRELATION ANALYSIS

Variable	Regression coefficient			
	Trial I	Trial II	Trial III	Trial IV
Solvent content	-167.38	-146.3	-109.4	-80.51
Ash content	408.95	OMIT	OMIT	OMIT
Percent Aromatics	-113.34	-100.02	-133.65	-117.84
Percent Ethers	-478.04	-492.21	-508.6	-392.57
Percent Nitrogen compounds	-434.63	-411.83	-328.8	OMIT
Percent Oxy acids	123.9	93.17	OMIT	OMIT
Constant term	2700.7	8414.3	8839.2	4976.97
Correlation coefficient	0.97	0.96	0.94	0.93

The final regression equation obtained is:

$$\mu = -80.51\ A\ -117.84\ B\ -392.57\ C\ +4976.97$$

where μ is the apparent viscosity in centipoises

A is the solvent weight percent of the sample

B is the percent aromatics in the sample

C is the percent ethers in the sample

This investigation of the rheological properties of SRL has helped in understanding the behavior of undeashed and deashed SRL and the relationship between viscosity and both process variables and sample properties. The information provided in this report should be useful from the standpoint of design of process equipment for handling SRL. Apparent viscosity measurements of undeashed SRL can also be used effectively as a process control variable. The apparent viscosity has been shown to have linear relations with temperature, melting point and solvent content, and non-linear relations with ash content and molecular weight average. Thus continuous on line viscosity measurements could provide information about the nature of the product in relation to its solvent content, ash content, melting point, or molecular weight average. Another point in favor of using apparent viscosity measurements is that no sample need be withdrawn for analyses. Thus results of apparent viscosity can be obtained at once and control of the process is thus enhanced.

Thus it can be concluded that apparent viscosity of SRL is a useful tool in monitoring process operation.

CHAPTER VIII

CONCLUSIONS

The following conclusions were drawn from the rheological study of solvent refined lignite (SRL) melts.

1. Deashed SRL approximates Newtonian behavior, and the viscosity is independent of shear rate. The deviations from the Newtonian behavior are greater at lower temperatures.

2. Undeashed SRL is non-Newtonian and shows a definite dependence of viscosity, with the apparent viscosity decreasing with increasing shear rate.

3. Both, the power law and the Bingham plastic model gave a good approximation to undeashed SRL melt behavior; the power law model gave a consistently better fit and is less influenced by temperature than the Bingham model.

4. The following statements were found true, about the behavior of the power law parameters.

a) The power law exponent 'n' changes only slightly with temperature.

b) The power law exponent 'n' increases monotonically with increase of ash content of the sample.

c) The power law exponent 'n' increases linearly with the increase in melting point of the sample.

d) The power law coefficient 'n' decreases monotonically with temperature.

5. The apparent viscosity of SRL (undeashed) at a particular shear rate decreases exponentially with increasing temperature. The temperature apparent viscosity relationship can be expressed mathematically as,

$$\mu = A\, T^{-B}$$

where A and B are non-negative constants,

μ is the apparent viscosity in centipoises

T if the absolute temperature in degrees Rankine.

6. The apparent viscosity of SRL has a linear relationship with its melting point, and increases with increase of melting point.

7. Increase of ash content increases SRL apparent viscosity. The relationship is exponential and can be expressed as

$$\mu = A \times W^{B}$$

where A and B are non-negative constants,

μ is the apparent viscosity in centipoises,

W is the ash content in weight percent.

8. Increase of molecular weight of SRL increases its apparent viscosity exponentially.

9. The apparent viscosity of SRL has an approximately linear relationship with its solvent weight content. Increase in solvent content reduces SRL apparent viscosity.

10. Samples investigated did not show a relation between the apparent viscosity and the solid density and process parameters such as solvent to coal ratio of feed and process conversion in the SRL pilot plant.

11. Preliminary investigation of SRL melts led to the following conclusions.

a. Temperature cycling has a hysteresis effect on the apparent viscosity of undeashed SRL.

b. Continuous shearing over extended periods of time increases the apparent viscosity of undeashed SRL.

c. Exposure of undeashed SRL to air during heating gave higher apparent viscosity readings than when nitrogen was used.

CHAPTER IX

SUGGESTIONS FOR FUTURE EXPERIMENTATION

The present study was essentially preliminary in nature and the area of rheology of solvent refined lignite melts needs further investigation.

It would be of interest to investigate the rheology of solutions of SRL in solvents such as anthracene, pyridine, or THF as this would be helpful in designing transportation facilities. The effect of temperature, solvent content, ash content, and solution density on the viscosity of SRL solutions would constitute a major part of such a study.

An important extension of the present study would be the investigation of the effect of additives on the viscosity of SRL. Particular attention should be given to those additives which have an effect of reducing the viscosity of SRL because of the industrial applicability of such a reduction on operation of the process. A detailed study of the effect of additives should include the variation of SRL viscosity with concentration and the properties of the additives.

The modeling of the behavior of SRL needs further study. The effect of solvent content, ash content and the molecular weight average on the power law parameters 'n' and 'm', in particular requires a detailed investigation.

The effect of temperature on SRL viscosity should be studied

over a wider range of temperatures. A study of the effect of each individual chemical constituent on the viscosity of SRL would be another avenue for investigation.

The effects of storage or aging on the viscosity of SRL should be studied at various temperatures. It is apparent that the viscosity increases during viscometric measurements at elevated temperature, and the viscosity may also increase during storage at ambient conditions.

APPENDIX A

TANGENTIAL ANNULAR FLOW OF A BINGHAM PLASTIC

The equation of motion for a Bingham plastic, between two concentric cylinders of inner radius r_1 and outer radius r_2 with the inner cylinder rotating at a constant speed, is

$$0 = \frac{1}{r^2} \frac{d}{dr}(r^2 \tau_{r\Theta}) \tag{A-1}$$

assuming the radial and vertical components of the velocity are zero, and that the angular component of the velocity is dependent on radius alone (6).

Equation (A-1) on integration and substitution of the boundary condition gives

$$\tau_{r\Theta} = \frac{T}{2\Pi hr^2} \tag{A-2}$$

The equation of state for a Bingham plastic is

$$\tau_{r\Theta} = -\mu_p \, r \, \frac{d}{dr}(v_\Theta/r) + \tau_o \tag{A-3}$$

where τ_o is the yield stress and μ_p is the plastic viscosity. Combining equation (A-2) and (A-3)

$$\frac{T}{2\Pi hr^2} = -\mu_p \, r \, \frac{d}{dr}(v_\Theta/r) + \tau_o \tag{A-4}$$

Equation (A-4) on rearrangement and integration gives

$$-\frac{T}{4\Pi hr^2} = -\mu_p \, (v_\Theta/r) + \tau_o \ln r + C_1 \tag{A-5}$$

Using the boundary condition $V_\Theta = 0$ at $r = r_2$

and substituting for the constant C_1 in equation (A-5), gives

$$-\frac{T}{4\Pi hr^2} = -\mu_p (v_\Theta/r) + \tau_o \ln r/r_2 - \frac{T}{4\Pi h r_2^2} \qquad \text{(A-6)}$$

Using the boundary condition $v_\Theta/r=\omega$ at $r=r_1$ and rearranging equation (A-6) yields

$$\omega = \frac{T}{4\Pi h\mu_p} (r_1^{-2} - r_2^{-2}) + \frac{\tau_o}{\mu_p} \ln r_1/r_2 \qquad \text{(A-7)}$$

For a Newtonian fluid equation (A-7) reduces to

$$\omega = \frac{T}{4\Pi h\mu_o} (r_1^{-2} - r_2^{-2}) \qquad \text{(A-8)}$$

TANGENTIAL ANNULAR FLOW OF A POWER LAW FLUID

Proceeding as in Appendix A and using the same assumptions, the equation of motion for a power law fluid reduces to

$$0 = \frac{1}{r^2} \frac{d}{dr} (r^2 \tau_{r\Theta}) \tag{B-1}$$

Integration and substitution of the boundary condition yields,

$$(\tau_{r\Theta})_{r = r_1} = \frac{T}{2\Pi\ hr_1^2} \tag{B-2}$$

The equation of state for a power law fluid is

$$\tau_{r\theta} = -m \left(r \frac{d}{dr} (v_\Theta/r)\right)^n \tag{B-3}$$

where 'n' is a dimensionless parameter and 'm' is a material characteristic parameter with units gm cm^{-1} sec^{-n} (6).

Combining equations (B-2) and (B-3) gives,

$$\frac{T}{2\Pi\ hr^2} = -m\left(r \frac{d}{dr} (v_\Theta/r)\right)^n \tag{B-4}$$

Equation (B-4) on integration gives,

$$v_\Theta/r = + (T/2\Pi hm)^{1/n} \cdot \frac{n}{2} \cdot r^{-2/n} + C_1' \tag{B-5}$$

Using the boundary condition $V_\Theta = 0$ at $r = r_2$

and substituting for C_1' in equation (B-5) yields,

$$v_\Theta/r = (T/2\Pi hm)^{1/n} \cdot \frac{n}{2} \cdot (r^{-2/n} - r_2^{-2/n}) \tag{B-6}$$

Using the other boundary condition, $v_\Theta/r = \omega$ at $r = r_1$, equation (B-6) yields,

$$\omega = (T/2\Pi hm)^{1/n} \cdot \frac{n}{2} \cdot (r_1^{-2/n} - r_2^{-2/n}) \qquad \text{(B-7)}$$

For a Newtonian fluid equation (B-7) reduces to

$$\omega = \frac{T}{4\Pi\, h\mu_o} (r_1^{-2} - r_2^{-2}) \qquad \text{(B-8)}$$

where μ_o is the Newtonian viscosity (absolute).

APPENDIX C

SAMPLE ANALYSES

TABLE 5

ANALYSIS OF SAMPLE I (PDU run SDR-5)[a]

Ash content (weight %) = 7.98%

Volatile matter (wt. %) = 50.33%

Fixed Carbon (wt. %) = 41.69%

Melting point = 214.8° F

Vacuum distillation at 1.6 Torr. Wt. % of solvent, heavy oil in sample[b]

Wt. % of 100°-230°C fraction (Solvent)	Wt. % of 230°C + fraction (Heavy Oil)	Wt. % of residue (by diff.) (SRL)
10.81	5.55	83.64

Pyridine soluble Wt. % (Ash free basis) = 59.33%

Heating value = 14,535 Btu/lb.

Elemental analysis: (Dry basis)

Carbon content = 80.5%

Hydrogen content = 5.39%

Sulfur content = 1.25%

Nitrogen content = 0.78%

Oxygen content (by difference) = 4.10%

[a] Run by the Project Lignite Laboratory in Grand Forks.

[b] 2:1 weight ratio of solvent to SRL sample used; distilled to smoke point. Based on distillate fractions corrected to 100 %.

TABLE 6

ANALYSIS OF SAMPLES OF GROUP II (PDU Run No. M-11)[a]

Yield Period	Ash Content (wt. %)	Volatile Matter (wt. %)	Fixed Carbon (wt. %)	Melting Point (°F)	Vacuum Distillation at 1.67 Torr[b] wt. fractions of solvent, heavy oil and residue			Pyridine soluble wt. % (Ash free basis)
					IBP-230°C (solvent)	230°C + Heavy Oil	Residue (by diff.)	
A	0.0	51.45	48.55	239	0	9.5	90.5	99.20
B	9.99	40.38	49.63	266	0	7.6	92.4	91.85
C	15.35	35.88	48.77	290	0	6.7	93.3	77.67
D	10.28	31.21	58.51	321	1.8	0	98.2	92.81

[a]Run by Project Lignite Laboratory, Grand Forks

[b]2:1 weight ratio of solvent to SRL sample used; distilled to smoke point. Based on fractions corrected to 100%.

TABLE 7

ELEMENTAL ANALYSIS OF SAMPLES FROM GROUP II

Yield Period	Carbon	Hydrogen	Nitrogen	Sulfur	Oxygen (by difference)
A	88.79	5.80	1.13	0.82	3.46
B	80.83	5.15	---	0.95	---
C	---	---	---	1.21	---
D	80.66	4.68	0.96	0.80	2.62

TABLE 8

ANALYSIS OF SAMPLES FROM GROUP III (Run No. M-29)[a]

Yield Period	Ash Weight %	Melting Point (°F)	Pyridine Solubility wt. % (ash tree)	Vacuum distillation at 1.6 Torr. wt. % of solvent, heavy oil and residue in F-1 sample[b]		
				Solvent (100-230° C)	Heavy oil 230° C +	Residue (by difference)
A	11.02	310	80.22	9.7	---	90.3
B	11.39	346	86.72	2.0	---	98.0
C	10.96	364	88.72	5.2	---	94.8
D	11.58	333	90.55	9.2	---	90.8
E	10.75	357	89.43	5.7	1.7	92.6
F	10.66	307	82.79	3.3	---	96.7
G	10.39	277	85.82	2.4	---	97.6
H	10.15	272	81.90	2.7	4.2	93.1
I	8.94	286	87.84	4.4	2.0	93.6

[a] Run by Project Lignite Laboratory, Grand Forks.

[b] 2:1 wt. ratio of solvent to SRL used. Distilled to smoke point.

TABLE 9

ELEMENTAL ANALYSIS OF SAMPLES FROM GROUP III

Yield Period	Carbon	Hydrogen	Nitrogen	Sulfur	Oxygen (by difference)
A	---	---	0.87	---	---
B	78.49	4.95	0.92	1.00	3.25
C	---	---	1.25	0.92	---
D	---	---	1.07	0.99	---
E	78.51	5.10	1.33	0.84	3.47
F	78.11	4.83	0.98	0.96	4.46
G	---	---	0.95	0.89	---
H	---	---	1.23	0.86	---
I	79.33	5.25	0.99	0.77	4.72

TABLE 10

ANALYSIS OF SAMPLES FROM GROUP IV (Run No. L-1)[a]

Code	Sample		Ash Wt. %	Melting Point °F	Pyridine Soluble Wt. % Ash Free
	Date	Time			
a	7-11-77	0930			
b	7-11	1400			
c	7-11	1700			
d	7-11	2100			
e	7-12	0130			
f	7-12	0500			
g	7-12	0900			
h	7-12	1300			
i	7-12	1700			
j	7-12	2100			
k	7-13	1700			
l	7-13	1900	11.54	244	97.73
m	7-13	2300	11.33	243	100.00
n	7-14	0700	10.72	264	98.25
o	7-14	1100	11.38	259	98.77
p	7-14	2300			
q	7-21	1100			

TABLE 10-- Continued

Code	Sample		Ash Wt. %	Melting Point °F	Pyridine Soluble Wt. % Ash Free
	Date	Time			
r	7-21	2300			
s	7-22	0530	12.99	324	83.64
t	7-22	0930	12.44	352	95.60

[a]Run by Project Lignite Laboratory, Grand Forks.

TABLE 11

SAMPLE GPLC ANALYSIS[a]

Sample	III A	III D	III G	III H	III I	IV L	IV N	IV R
% Nonvolatile	94.10	93.76	86.56	79.34	86.41	86.87	89.52	86.10
% Soluble THF	70	72	80	79	81	69	84	87
Mol. wt. w/solvent	725	848	720	786	811	874	789	713
Mol. wt. w/o solvent	777	895	793	875	898	975	873	823
% frac. 1	0	.37	0	.22	.53	0	0	.30
% frac. 2	2.66	8.52	12.59	5.49	9.38	6.25	5.71	15.42
% frac. 3	5.21	2.02	3.86	4.84	4.81	5.35	7.77	3.01
% frac. 4	9.14	10.03	10.03	7.59	8.49	8.02	7.74	7.84
% frac. 5	18.84	19.67	21.52	21.69	25.89	16.12	20.55	18.06
% residue	64.15	59.39	52.00	55.24	54.79	59.93	57.24	55.37
% frac. 1 and 2	2.66	8.89	12.59	10.64	6.02	10.58	6.25	15.72

frac. 1 contains aliphatics; frac. 2 aromatics; frac. 3 ethers; frac. 4 nitrogen compounds; frac. 5 oxygen acids; and frac. 6 highly polar materials.

[a]Prepared by Grand Forks Energy Research Center

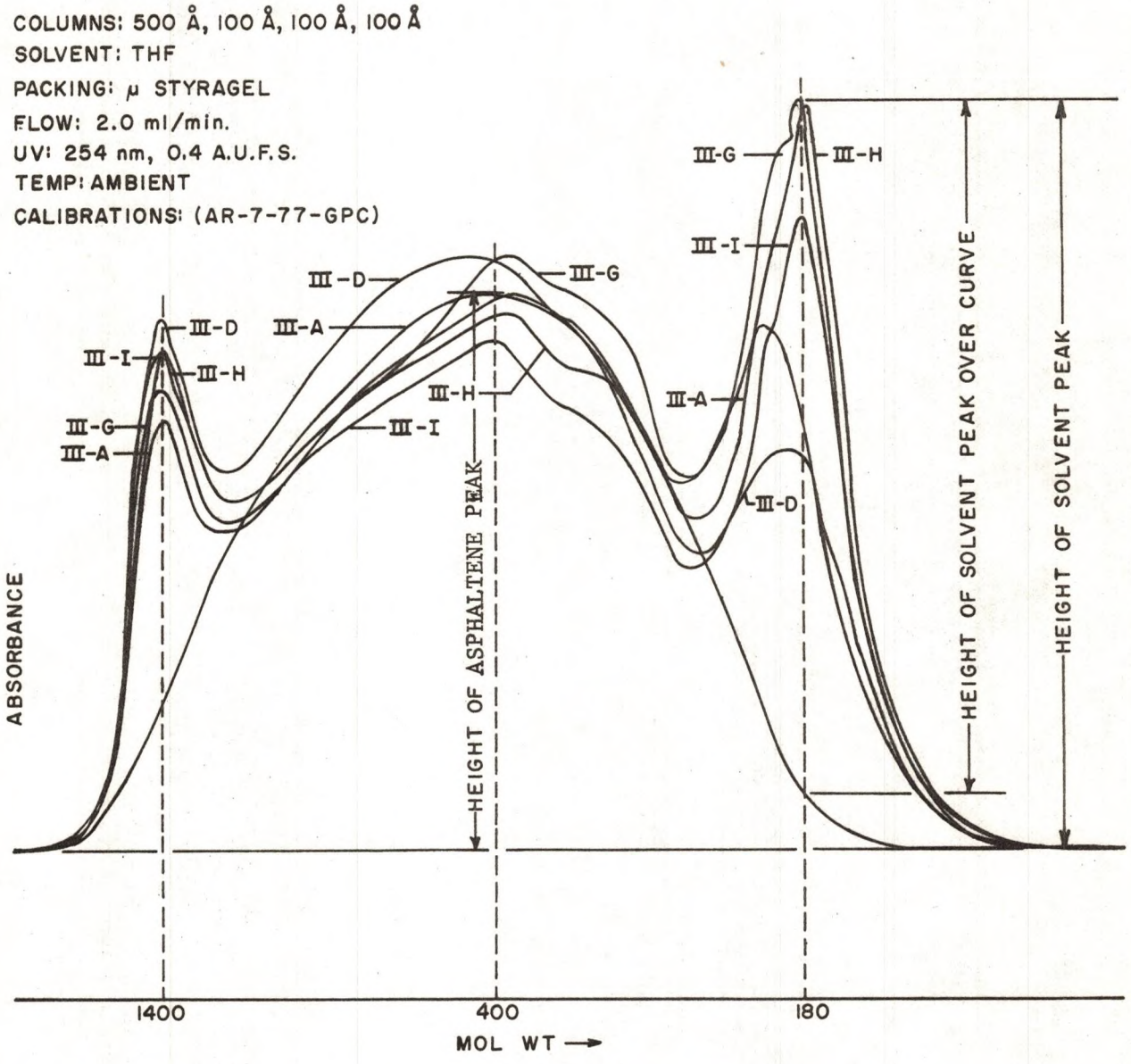

FIGURE 34- MOL WT DISTRIBUTION OF SRL SAMPLES (GROUP III)

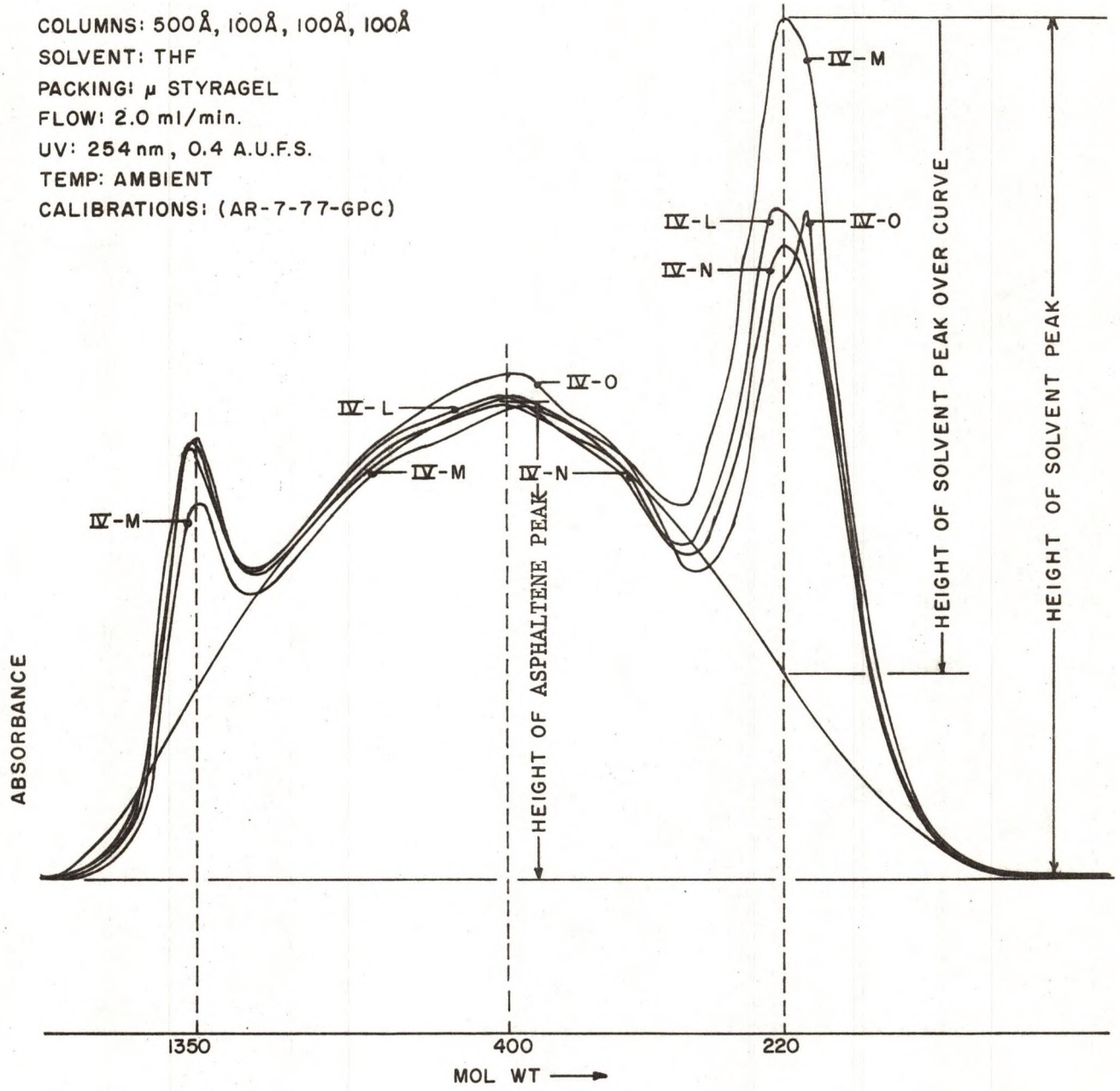

FIGURE 35 - MOL WT DISTRIBUTION OF SRL SAMPLES (GROUP IV)

APPENDIX D

SPECIFICATIONS OF INSTRUMENTS USED

The Thermosel System used consists of three basic components:

1. A thermo-container
2. An SCR temperature controller
3. A Brookfield Synchro-Lectric Viscometer

1. Thermo container

Manufacturers: Brookfield Engineering Laboratories, Inc.
Stoughton, MA USA

Accessories:
1. Removable Sample Chamber
2. Insulating Cap
3. Cooling plug with tubing
4. Extracting tool
5. Sample Chamber holder

Maximum temperature limit: 595°F

Power Supply: 110 volts AC, Frequency - 60 Hertz

2. Temperature controller

Manufacturer: Brookfield Engineering Laboratories
Stoughton, MA USA

Model: Model 63-A

Lower limit of precise control: 20°F above ambient

Upper limit of precise control: 500°F

Description: The proportional temperature controller is designed to maintain an accurate, non fluctuating temperature of the electrically heated Thermo-container. Temperature is measured by a platinum resistance temperature detector (RTD) and power to the electrical heating element is smoothly regulated by the controller to the level necessary to maintain this temperature.

Temperature is set by a set point dial on the front of the instrument. As set-point temperature is approached, power is reduced to a level which will sustain this temperature. If set point dial is rotated up or down the controller will supply increased or reduced power to bring the temperature of the platinum sensor to the new control point.

The proportional band adjustment determines the sensitivity of the unit. At minimum proportional band setting, the gain of the controller is maximum and output power will be controlled between 0% and 80% as a result of approximately a 1.0°F temperature deviation. With wide proportional band setting (minimum gain) this change will occur as a result of approximately a 10.0°F temperature deviation.

Specification: Electrical resistance load - 1000 watts at 120 volts.
Resistance of the platinum RTD probes - 100 ohms at 0°C
Accuracy of set point - ± 0.25% of the nominal sensor wave.
Fuses - should carry 100% of rating, open at 1000 seconds or overloads between 120% and 180% of rating; open within 1 second at 250% of rating.

3. Synchro-Lectric Viscometer

Manufacturers: Brookfield Engineering Laboratories, Inc.
Stoughton, MA USA

Name of Instrument and Model: Brookfield Synchro-Lectric Viscometer Model LVT with speeds 60,30,12,6,3,1.5,0.6 and 0.3 RPM

Accessories:
1) Laboratory Stand, Model A
2) Alignment bracket
3) Spindles SC4-18, SC4-31, SC4-34

Specifications: Full scale torque - 673.7 dynes cm.
Torque versus dial reading in a linear relationship.
The viscometer is accurate to within 1% of full scale when centered in a container over 2'75" in. dia.

BROOKFIELD THERMOSEL RANGE DATA

Spindle	Viscosity Range (CPS)	Shear Rate (Sec^{-1})	Sample Volume (cc)
SC4-18	5-10,000	1.32N*	8.0
SC4-31	50-100,000	0.34N	10.0
SC4-34	100-200,000	0.28N	9.5

* N = RPM

Note: For each range the first number represents the minimum recommended measurable viscosity (10% of the lowest full scale range of the viscometer).

TABLE 12

BROOKFIELD THERMOSEL SPINDLE FACTORS[a]

Speed (RPM)	LV Series Spindle Number		
	SC4-18	SC4-31	SC4-34
60	0.5	5	10
30	1	10	20
12	2.5	25	50
6	5	50	100
3	10	100	200
1.5	20	200	400
0.6	50	500	1000
0.3	100	1000	2000

To calculate viscosity in centipoise (CPS) multiply the dial reading by the factor corresponding to the viscometer spindle and speed combination utilized.

[a] Supplied in manufacturers brochure.

APPENDIX E

SAMPLE DATA FOR A PARTICULAR MEASUREMENT

TABLE 13

SAMPLE EXPERIMENTAL DATA

Sample Weight: 10 gms.

Temperature: 440°F

Spindle No.: SC4-34

RPM	Dial reading	Factor	Viscosity (CPS)	Mean Viscosity
30	93.0	20	1900	
30	92.0	20	1800	1850
30	92.5	20	1850	
12	46.0	50	2300	
12	46.0	50	2300	2300
12	46.0	50	2300	
6	27.0	100	2700	
6	27.0	100	2700	2700
6	27.0	100	2700	
3	16.5	200	3300	
3	16.0	200	3200	3250
3	16.25	200	3250	

Specific gravity measurement of the solid sample:

Weight of empty S.G. bottle (w_1) = 13.89 16 gm.
Weight of S.G. bottle + solid (w_2) = 14.4874 gm.
Weight of S.G. bottle + solid (w_3) = 34.2866 gm.
+ kerosene

Weight of bottle + kerosene only (w_4) = 34.0583 gm.

Weight of bottle + water only (w_5) = 38.9182 gm.

Calculations

Weight of solid = $w_2 - w_1$ = 0.5958 gm.

Weight of an equal volume of kerosene = $(w_4-w_1) - (w_3-w_1)-(w_2-w_1)$

= $(w_4-w_3)-(w_2-w_1)$ = 0.3675 gm.

Sp. gr. of solid with respect to kerosene = $\frac{0.5958}{0.3675}$ = 1.6212

Sp. gr. of kerosene = $(w_4-w_1)/(w_5-w_1)$ = 0.8058

Sp. gr. of solid = (1.6212)(.8058)

= 1.3064

APPENDIX F

COMPLETE APPARENT VISCOSITY DATA

TABLE 14

APPARENT VISCOSITY DATA FOR SAMPLE I

RPM	Apparent Viscosity (in cps)	
	440°F	500°F
30	1850	1250
12	2300	1570
6	2700	1900
3	3250	2500

TABLE 15

APPARENT VISCOSITY DATA FOR SAMPLE II

RPM	Apparent Viscosity (in cps)		
	350°F	400°F	450°F
60	238	68.3	25
30	223	66.6	25
12	218	66.6	25

TABLE 16

APPARENT VISCOSITY DATA FOR SAMPLE III

RPM	Apparent Viscosity (in cps)							
	A	B	C	D	E	G	H	I
0.6	7000	9500	10500	9000	8000	---	---	7000
1.5	4800	5800	6500	5100	4800	---	---	4200
3	3400	3900	4200	4600	4100	360	400	2750
6	2300	3100	3350	3600	3700	300	305	2000
12	1700	3000	2850	3100	3200	275	300	1375
30	---	---	---	---	---	250	280	---

TABLE 17

APPARENT VISCOSITY DATA FOR SAMPLE IV

RPM	Apparent Viscosity (in cps)															
	A	B	C	D	E	F	G	H	I	J	K	L	M	N	O	P
60	230	160	120	200	240	210	220	.90	170	165	150	200	160	220	340	265
30	310	180	160	250	305	270	300	110	200	230	190	280	200	290	460	330
12	375	275	250	350	475	337.5	425	125	237.5	325	225	400	275	375	525	450

TABLE 18

EFFECT OF TEMPERATURE CYCLING ON APPARENT VISCOSITY (SAMPLE II)

RPM	Apparent viscosity (cps)					
	400°F	350°F	400°F	350°F	400°F	350°F
12	87.5	312	100	340	147.5	375
30	80.0	280	90	295	103.0	315
60	77.5	272	80	280	81.0	295

TABLE 19

EFFECT OF CONTINUED SHEARING OVER EXTENDED PERIODS OF TIME (SAMPLE III-A) T = 500°F

Time (min)	0	15	20	25	30	35	40	45	60	80
Apparent viscosity (cps)*	--	4250	3650	3198	3140	3128	3115	3110	3108	3110

Time (min)	100	160	205	220
Apparent viscosity (cps)	3115	12000	80000	6000000

* Note: Continuous shearing done at 60 rpm: Apparent viscosity measurements made at 12 rpm. Different spindle used to permit high viscosity measurements in the last three readings.

TABLE 20

EFFECT OF AIR EXPOSURE ON APPARENT VISCOSITY (SAMPLE III-E)

$T = 500^{\circ}F$

RPM	Apparent viscosity (cps)	
	With nitrogen blanketing	Without nitrogen blanketing
0.6	8,000	10,000
1.5	4,800	6,800
3.0	4,100	5,300
6.0	3,700	4,200
12.0	3,200	3,400

TABLE 21

EFFECT OF TEMPERATURE ON APPARENT VISCOSITY (SAMPLE IV-T*)

RPM	Apparent viscosity (cps)						
	$350^{\circ}F$	$375^{\circ}F$	$400^{\circ}F$	$425^{\circ}F$	$450^{\circ}F$	$475^{\circ}F$	$500^{\circ}F$
60	---	---	---	---	840	510	400
30	---	---	---	1350	1020	770	520
12	---	---	2550	1575	1375	850	700
6	---	5700	2750	1750	1700	1400	1050
3	16600	7000	3000	2100	1900	1700	1400
1.5	20600	8600	3700	---	---	---	---
0.6	27500	14000	---	---	---	---	---
0.3	41000	---	---	---	---	---	---

*Shear rate (Sec^{-1}) = 0.28N where N is the rpm.

APPENDIX G

SAMPLE CALCULATION OF TORQUE AND ANGULAR VELOCITY

From Table 9, for Sample I at 440°F and 30 rpm, the apparent viscosity is 1850 centipoises (cps). The angular velocity (ω) corresponding to a speed of rotation of 30 rpm is given by:

$$\omega = \frac{30}{60} \cdot 2\Pi = \Pi \text{ rad. sec}^{-1}$$

The torque is calculated using equation (3.4) as follows,

$$T = \frac{4 \Pi \ h \ \mu\omega}{(r_1^{-2} - r_2^{-2})}$$

Using the values h = height of the inner cylinder = 2.5 cm

μ = apparent viscosity = 18.5 poises

r_1 = radius of the inner cylinder = 0.5 cm

r_2 = radius of the outer cylinder = 1.0 cm

ω = angular velocity = Π rad. sec^{-1}

we get, Torque (T) = 608.6 dyne cm.

The table below gives the calculated values of torque and angular velocity for Sample I, at 440°F

RPM	Apparent Viscosity (cps)	Angular Velocity (Rad. Sec^{-1})	Torque (Dynes cm)
30	1850	Π	608.6
12	2300	$2\Pi/5$	302.6
6	2700	$\Pi/5$	177.6
3	3250	$\Pi/10$	106.9

These values are plotted in the torque-angular velocity relationship diagram for this sample in Figure 9.

APPENDIX H

TORQUE - ANGULAR VELOCITY DATA

TABLE 22

TORQUE - ANGULAR VELOCITY DATA FOR SAMPLE I

Angular Velocity (rad. sec^{-1})	Torque (dyne cm)	
	$440^{o}F$	$500^{o}F$
Π	608.6	420.6
0.4Π	302.6	211.3
0.2Π	177.6	127.9
0.1Π	106.9	86.1

TABLE 23

TORQUE - ANGULAR VELOCITY DATA FOR SAMPLE II

Angular Velocity (rad. sec^{-1})	Torque (dyne cm)		
	$350^{o}F$	$400^{o}F$	$450^{o}F$
2Π	160.2	46.0	16.8
Π	150.0	22.4	8.4
0.4Π	146.7	8.9	3.3

TABLE 24

TORQUE - ANGULAR VELOCITY DATA FOR SAMPLE III

$T = 500^{o}F$

Angular Velocity (rad. sec^{-1})	Torque (dyne cm)							
0.02Π	47.1	63.9	70.6	60.5	53.8	---	---	47.1
0.05Π	81.6	97.5	109.3	85.8	81.6	---	---	70.6
0.10Π	114.4	131.2	141.3	154.8	137.9	12.1	13.4	92.5
0.20Π	154.8	208.6	225.6	242.3	249.0	20.2	20.2	134.7
0.40Π	229.5	404.2	383.6	417.2	430.7	37.0	40.3	185.2
Π	---	---	---	---	---	84.1	94.2	---

TABLE 25

TORQUE - ANGULAR VELOCITY DATA FOR SAMPLE IV-T

Angular Velocity (rad. sec^{-1})	Dial Reading (Torque/6.73)						
	350°F	375°F	400°F	425°F	450°F	475°F	500°F
2Π	---	---	---	---	84.0	51.0	40.0
1Π	---	---	---	67.5	51.0	33.5	26.0
0.4Π	---	---	51.0	31.5	27.5	19.0	14.0
0.2Π	---	57.0	27.5	17.5	17.0	14.0	9.5
0.1Π	83.0	34.0	15.0	10.5	9.0	8.2	7.0
0.05Π	51.5	21.5	9.2	6.5	---	---	---
0.02Π	27.5	12.5	5.2	---	---	---	---
0.01Π	18.0	8.0	---	---	---	---	---

APPENDIX I

CALCULATION OF POWER LAW PARAMETERS

Theory:

The relationship between torque (T) and angular velocity (ω) for a power law fluid is given in equation (3.6) as,

$$\omega = \left(\frac{T}{2\Pi hm}\right)^{1/n} \cdot \frac{n}{2} \cdot \left(r_1^{-2/n} - r_2^{-2/n}\right) \qquad \text{(I-1)}$$

This equation can be rearranged to give,

$$T = 2\Pi hm \left(\frac{2\omega}{n(r_1^{-2/n} - r_2^{-2/n})}\right)^n \qquad \text{(I-2)}$$

Taking logarithms on both sides of the above equation,

$$\log T = n \log \omega + I \qquad \text{(I-3)}$$

where 'n' is the slope of the log T versus log plot, and

I is the intercept of the plot given by,

$$I = n\log \frac{2}{n(r_1^{-2/n} - r_2^{-2/n})} + \log_{(2\Pi hm)} \qquad \text{(I-4)}$$

The value of 'm' can be calculated from equation (I-4) to be,

$$m = \frac{1}{2\Pi h} 10^{\left(I - n\log \frac{2}{n(r_1^{-2/n} - r_2^{-2/n})}\right)} \qquad \text{(I-5)}$$

Thus the power law parameters 'n' and 'm' can be calculated from the slope and intercepts of the log T versus log ω plot.

Sample calculation:

The values of torque and angular velocity for sample IV-T at 350°F, plotted in Figure 14, are shown in the table below.

TABLE 26

SAMPLE CALCULATIONS OF TORQUE-ANGULAR VELOCITY

Dial reading	RPM	T (dyne cm)	ω (rad. sec^{-1})	log T	log ω
18.0	0.3	121.1	0.01	2.08	-1.5
27.5	0.6	185.0	0.02	2.26	-1.2
51.5	1.5	346.6	0.05	2.53	-0.8
83	3.0	558.6	0.1	2.75	-0.5

The torque and angular velocity were calculated from the dial reading and rpm, respectively, using the method in Appendix G. A plot of log T versus log ω on cartesian co-ordinates, for this sample, yielded a slope (n) of 0.668, and an intercept (I) of 3.072. The value of 'm' was calculated using the value of I in equation (I-5) to be 132.09.

In the same manner, the power law parameters 'n' and 'm' were calculated for the other temperatures. The table below summarizes the calculated values of 'n' and 'm' for sample IV-T at different temperature.

TABLE 27

CALCULATED VALUES OF POWER LAW PARAMETERS

Temp. (^{o}F)	'n'	I	'm'
350	0.668	3.072	132.09
375	0.647	2.698	56.46
400	0.763	2.427	28.50
425	0.784	2.252	18.85
450	0.730	2.178	16.73
475	0.595	2.066	13.55
500	0.592	1.943	10.23

These values of 'n' and 'm' are plotted as a function of temperature in Figures 21 and 22 respectively.

Verification:

Using the values of n = 0.668, m = 132.09, r_1 = 0.5, r_2 = 1.0 and h = 2.5 we get the following relationship between torque (T) and angular velocity (ω), for sample IV-T at 350°F,

$$\omega = 2.510^{-5} (T)^{1/\ 0.668}$$

Now, any value of T from the table on the previous page when used with above equation should result in the corresponding ω. For example, using a value of T = 185.0 yields a value of ω = 0.0620 rad. $sec.^{-1}$. Actual value of ω from the table is 0.2 or .0628 rad. $sec.^{-1}$.

1. Hottel, H.C. New Energy Technology - Some Facts and Assessments, Cambridge, Mass: The MIT Press, 1977.

2. Solutions to Sticky Problems, Stoughton, Mass: The Brookfield Engineering Laboratories, n.d.

3. Van Waser, J.R., Lyons, J.W., Kim, K.Y., and Colwell, R.E. Viscosity and Flow Measurement, New York: Interscience Publishers, 1963.

4. Bird, R.D., Steward, W.E., and Lightfoot, E.V. Transport Phenomena, New York: John Wiley and Sons, Inc., 1960.

5. Shaheen, E.I. "Rheological Study of Viscosities and Pipeline Flow of Concentrated Slurries," Ph.D. Dissertation, University of Tennessee, 1967.

6. Mishra, R.N. "Rheological Study of Concentrated Silica Suspensions", Masters Thesis, University of North Dakota, 1969.

7. Brodkey, R.S. The Phenomena of Fluid Motions, Reading, Mass: Addison-Wesley Publishing Company, 1967.

8. Huang, H., Fischer, J. "Laboratory Studies for Separation of Solids from Synthoil Gross Product," Argonne National Laboratory, ANL-76-91, November, 1976.

9. Physical and Chemical Behavior of Liquified Coal in Solids Separation, Quarterly Report, Ann Arbor, Mich: University of Michigan, Oct.-Dec., 1976.

10. Knell, E.W., Gethard, P.E., Shaw, B.W., Green, N.W., and Quader, S.A. Flash Pyrolysis Coal Liquefaction Process Development, LaVerne, California: Occidental Research Corporation, February, 1977.

11. Klunder, E.B., Zielke, C.W., Maskew, J.T., Parter, W.A., Pell, M., and Struck, R.T. Zinc Halide Hydrocracking Process for Distillate Fuels from Coal, Library, Penn: Conoco Coal Development Company, n.d.

12. Sternberg, H.W., Raymond, R., and Schweighardt, F.K. "Viscosity of Petroleum Heavy Ends." Science 188, 1975, p. 49.

13. Burk, E.H. Jr., and Kulta, H.W. "Molten Asphaltene Viscosities." Coal Chem. Workshop, Menlo Park, CA: Stanford Res. Inst., August, 1977.

14. Moschopedis, S.E., Fryer, J.F., and Speight, J.G. "Solution Viscosity of Athasbaca Asphaltenes." Fuel 55, 1976, p. 227.

15. Schiller, J.E., Farnum, E.W., and Sondreal, E.A. "Viscosity of Coal Liquids." Production of Liquid Fuels From Coal, Chicago, IL: ACS Div. of Fuel Chemistry, Sept. 1977.